OPEN ACCESS

Remote Sensing

Article

LIDAR and SODAR Measurements of Wind Speed and Direction in Upland Terrain for Wind Energy Purposes

Steven Lang * and Eamon McKeogh

Department of Civil and Environmental Engineering, University College Cork, Cork, Ireland;
E-Mail: e.mckeogh@ucc.ie

* Author to whom correspondence should be addressed; E-Mail: steve@westwind.ie;
  Tel.: +353-21-439-4291; Fax: ++353-21-439-4291.

Abstract: Detailed knowledge of the wind resource is necessary in the developmental and operational stages of a wind farm site. As wind turbines continue to grow in size, masts for mounting cup anemometers—the accepted standard for resource assessment—have necessarily become much taller, and much more expensive. This limitation has driven the commercialization of two remote sensing (RS) tools for the wind energy industry: The LIDAR and the SODAR, Doppler effect instruments using light and sound, respectively. They are ground-based and can work over hundreds of meters, sufficient for the tallest turbines in, or planned for, production. This study compares wind measurements from two commercial RS instruments against an instrumented mast, in upland (semi-complex) terrain typical of where many wind farms are now being installed worldwide. With appropriate filtering, regression analyses suggest a good correlation between the RS instruments and mast instruments: The RS instruments generally recorded lower wind speeds than the cup anemometers, with the LIDAR more accurate and the SODAR more precise.

Keywords: wind speed; wind energy; remote sensing; upland terrain

1. Introduction

1.1. Rationale

An intimate knowledge of a site's wind resource is essential for many aspects of wind energy development, including site finding in the pre-development phase, resource assessment, wind flow modeling, turbine micrositing and wind farm energy yield optimization in the development phase, and power curve verification, wind-induced load measurements and for insurance purposes in the operational phase.

Wind monitoring for these wind energy purposes has, to date, relied on the cup anemometer as the de facto standard [1], mainly due to the technology and the measurement uncertainties being so well understood (e.g., [2,3]). A cup anemometer requires mounting on a mast that must be at or near the hub height of the wind turbine for which the site is to be developed for, and this mast must be located in a location that represents the wind flow over the site and which is not impeded by obstacles or terrain features that distort the flow at the point location of the cup anemometer.

However, with the ever-increasing development of physically larger wind turbines (both in hub height and rotor diameter), the need for taller and taller masts (and multiple masts for the larger sites now being developed) is adding both significant cost and risk to projects, particularly those in the early stages, prior to financing. Planning impacts, cost and the physical limitations of masts have led to decreasing rewards for continuing higher than about 80–100 m. The need for more flexible methods of monitoring wind is therefore clear.

1.2. Remote Sensing

The two remote sensing (RS) techniques used to date in wind energy applications are LIDAR (LIght Detection And Ranging, or 'laser radar') and SODAR (SOund Detection And Ranging, or 'acoustic radar'). Both techniques employ the Doppler effect to detect the movement of air in the atmospheric boundary layer (ABL) and infer wind speed and direction: In the case of LIDAR, electromagnetic radiation is reflected off particles, whereas with SODAR a pulse of sound is reflected off the varying temperature structure in the atmosphere.

Both SODAR and LIDAR remote sensing methods have increasingly been applied in wind energy research projects, as well as in support of the commercial development of wind farms (both on and offshore), over the past decade. These methods allow an efficient means of detailed mapping of the wind fields around potential sites, as well as the only practical way of measuring the change of wind speed, or shear, across the entire rotor disc of a large modern wind turbine, due to the limitations—and cost—of such tall masts as would span the full tip height of modern tall turbines (up to 200 m for the tallest turbine tip height installed to date).

Because these techniques, by their nature, measure the wind field over a much larger volume than that of a cup anemometer, their application for measuring wind speeds over terrain where large spatial variations may occur (such as in upland areas or where obstacles are significant) has been shown to be less predictable than cup anemometry to date.

Cup anemometers mounted on carefully located tall masts are therefore still the standard for financing of wind projects and power curve verification. With regards to project financing

requirements, the due diligence process relies on the 'stress testing' of financial models. This involves using uncertainties associated with estimations of a site's wind energy yield to calculate various probabilistic levels of energy output and corresponding financial rates of return. With current uncertainty in the accuracy and repeatability of wind measurements using RS, further development of the instrumentation and data processing methods is an important step in increasing confidence in these techniques.

Most studies to date on the use of RS for wind energy applications have been carried out in simple terrain. Therefore, an important aspect of this research was to investigate how well LIDAR and SODAR can measure the wind in more complex, upland terrain.

1.2.1. SODAR Background

A SODAR is a ground-based remote sensing instrument that transmits (via speakers) a short acoustic sinusoidal pulse (typically 50 ms) into the ABL, then listens for return signals for a short period of time, measuring the sound waves that are scattered back by turbulence caused by the thermodynamic structure of the atmosphere. Both the intensity and the Doppler shift of the returns can be used to determine wind speed and direction and the turbulent structure of the lower atmosphere, up to about 2 km (depending on the system's power output, sonic frequency, atmospheric stability, turbulence and the existing noise environment). SODARs consisting of 3 or more beams at different angles to the vertical allow a three-dimensional vertical wind profile to be obtained. The most typical topology is that of the 'mono-static' SODAR, where the transmitter and receivers are all co-located in a relatively compact unit. The theoretical basis of the SODAR technique and its practical application has been detailed in [4].

The monostatic SODAR equation is given by [5]:

$$P(R) = P_0 \, AL \, \sigma(R) \, exp(-2\alpha R)/R^2 \qquad (1)$$

where:
$P(R)$ is the power received from distance R,
P_0 is the effective transmitted power,
A is the effective area of the receiver,
L is the length of the acoustic pulse in space and
σ is the acoustic reflectivity (backscattering cross-section) at distance R. The exponential is the transmission term (which can vary between 0 and 1), where α is the average molecular attenuation coefficient of sound in air over the distance R and the factor 2 provides for the two-way transmission path.

SODAR is useful in studying special meteorological phenomena such as atmospheric dispersion of pollutants, sound transmission and vortex generation (for aircraft warning). A description of its scientific basis and the various applications in which it has been employed (before the specific application to wind energy) can be found in [6-8]. A 1998 review of Doppler SODAR performance noted that, up to that time, little work had been carried out on comparing the various commercially available SODARs with data from nearby instrumented meteorological masts [9].

1.2.2. LIDAR Background

A LIDAR is an active optical remote sensing instrument that transmits a laser beam (either as a continuous wave, or as a pulse) into the ABL and measures the scattered radiation received back at the instrument. It can be deployed both at ground level and airborne, for different applications. The technique has been in use for decades and descriptions can be found in numerous texts (e.g., [10-12]). LIDARs can use radiation in the ultraviolet, visible and infrared regions of the electromagnetic spectrum, and each of these will interact differently with the various physical processes within the atmosphere. Thus the choice of differing scattering processes allows an array of information about the ABL to be inferred, such as temperature, atmospheric composition and wind (e.g., [13-15]). The small divergence of the laser beam results in a very low beam width (and hence volume) up to a few hundred metres for a continuous wave (cw) LIDAR (such as used in this study), and up to tens of kilometers for pulsed LIDARs, allowing high resolution even at these heights [16]. The former systems rely on detector focusing to resolve vertical distance, while the latter uses signal timing.

In simple terms, the backscattered LIDAR signal can be described as [12]:

$$P(R) = K \, G(R) \, \beta(R) \, T(R) \tag{2}$$

where:
K is the performance of the system,
$G(R)$ is the range-dependent geometric factor,
$\beta(R)$ is the backscatter coefficient at distance R and
$T(R)$ is the transmission factor, which describes how much light is lost from the LIDAR to distance R and back.

1.3. Remote Sensing for Wind Energy Applications—Review of Research

1.3.1. SODAR Studies

The earliest utilization of RS methods for wind energy was in the study of wakes behind large wind turbines, measuring turbulence structure with a SODAR, in the late 1980s [17,18]. Early on-shore comparisons between SODARs and instrumented met masts were reported with varying degrees of success and with observations on the limitations of the technology available at the time (e.g., [19-21]).

Intense interest in offshore wind development and the added difficulty—and cost—of establishing tall, instrumented masts at sea, initially led to a number of studies using ship-mounted SODARs in the early 2000s. Velocity deficit measurements behind offshore wind turbines were reported in [22,23], allowing the development of empirical models of offshore wakes Output from these models were compared to SODAR measurements in [24].

Intercomparisons on three phased-array SODARs were described in [25,26] and it was concluded that filtering of results and the calibration method employed were the major issues for SODARs being used for wind energy applications.

The EU WISE (WInd energy SODAR Evaluation) project, in 2005, determined a SODAR calibration technique for wind energy applications and identified the main sources of measurement error, resulting in increased confidence in the method within the wind energy industry [27]. This study

also found no difference between the root-mean-square residuals of SODAR-mast and mast-mast data (different cup anemometers on the same mast), except at higher wind speeds (>11 m/s). Because of the sensor separations (SODAR and cup anemometer, 70 m; compared to cup anemometers, 20 m), the researchers surmised that the sensors were not necessarily exposed to the same wind stream, implying that the SODAR was measuring wind speed to at least as high a reliability as the cup anemometers [27].

The problem with SODAR of deteriorating signal-to-noise ratio (SNR) for increasing height and wind speed was highlighted in [28], which suggested that classical (cup anemometer) measurements were still needed to provide accurate wind resource assessment.

In 2008, a scanning *bi-static* SODAR was described, in which transmitters and receivers are spatially separated by (ideally) tens of meters [29]. This allows much better accuracy in complex terrain, as it samples a single compact volume of air, rather than transmitting in widely separated directions (as in a mono-static SODAR, where the transmitter and receiver are co-located). Bradley *et al.* [4,30] further described these "next-generation" bi-static pulsed SODARs now emerging, and their advantages, such as improved SNR (through pulse-coding signal processing enhancements), better range, lower data scatter and, compared to LIDARs, significantly lower power requirements and cost.

In the US, in 2010, an intercomparison study of data from a met tower (80 m) and a new American SODAR design now commercially available ('Triton') was described in [31]. Results showed good correlation for wind speed and wind direction up to 80 m, with a 2% difference between average wind speed from the SODAR and cup anemometers. A consistent discrepancy in average turbulence intensity (TI) was observed (about 40% lower in the SODAR data). However, the source of this was not clear, as the SODAR values were consistent with Great Plains TI values. The results were in broad agreement with those found in [32], for the same SODAR against an instrumented 108 m mast at a coastal test site in the Netherlands (including the significantly lower TI recorded by the SODAR).

1.3.2. LIDAR Studies

Development of LIDARs for use in the lowest levels of the ABL for wind energy purposes occurred later than that of SODARs. In 2004, a comparison between a newly developed continuous wave (cw) LIDAR ('ZephIR') and cup anemometry up to 100 m was carried out [33]. This study explained the offset observed between LIDAR and cup anemometer measurements as due to laser calibration at too short a range and beam focusing due to curvature on "flat" optical surfaces. While they contended that each measurement of velocity with LIDAR was accurate and reliable, errors arose because of the uncertainty of what is actually moving at that velocity. They questioned the assumption that the backscattered signal always only originates from aerosols moving at the wind speed close to beam focus. Non-uniform backscatter can occur, e.g., from cloud or mist, as contributions from the Doppler signal from the cloud or mist layer base can contaminate that from aerosols at the height being measured. These effects could increase due to low cloud or mist layer height, high LIDAR range setting and low aerosol scattering at focus. In the worst case, the return signals from a cloud base could dominate those from aerosols at the desired height, leading, in many instances to an overestimation of wind speed. Hence a cloud correction algorithm is necessary.

Deutsche WindGuard Consulting [34] also evaluated the ZephIR LIDAR and reported good comparison with cup anemometer data when the LIDAR's 'cloud correction' was applied. Without this correction, there were unacceptably high misinterpretations of wind speed during periods of low wind shear and high cloud cover.

A comprehensive uncertainty analysis of both ZephIR LIDAR data and cup anemometer data in a US validation study (up to a height of 118 m) in flat terrain indicated a LIDAR error in wind speed measurement of about 5%, compared to about 8% from the anemometers [35]. The reason for the larger cup error calculated was that the anemometer used was a *generic* model and not IEC certified. One of the main motivations was to quantify all the known uncertainties in both LIDAR and cup anemometers, and they identified seven for the cup data, and nine for the LIDAR. Other intercomparison studies have used higher specification (and MEASNET calibrated) anemometers and therefore typically reported these as the standard against which the LIDAR was measured.

In 2007, an on-shore comparison of the QinetiQ ZephIR LIDAR beside a 120 m instrumented mast, followed by a 3-month campaign on the FINO-1 research platform in the North Sea off the German coast was described in [36]. This platform is 20 m above sea level (a.s.l.), on which is mounted an 80 m instrumented mast, with top-mounted cup anemometry at 103 m a.s.l. LIDAR *versus* mast regression slopes were shown to decrease with height, although correlation coefficients were close to 1. These results were considered anomalous in [37], which noted that LIDAR performs similarly to SODAR and with comparable uncertainty, particularly if the LIDAR results are normalized to the results from a cup anemometer at a fixed height. It was contended that the main limitation to the accuracy of the ZephIR in flat terrain was probably the leveling of the instrument, and that even though its large beam (zenith) angle results in lower tilt errors, these were still likely to be the cause of the systematic deviations evident in the data of [36].

A pulsed Doppler LIDAR designed for wind energy applications ('Windcube') was introduced to the wind energy industry in 2007. Albers *et al* [38] reported on a measurement campaign including both the ZephIR and Windcube, in flat terrain at a northern German test center. Both LIDARs performed well, with data availabilities over 96% at 124 m height and LIDAR-cup standard deviation errors of 0.24 m/s (Windcube) and 0.3 m/s (ZephIR). [39] summarised a number of other Windcube measurement campaigns. Against cup anemometers, these showed linear regression slopes in flat terrain of 0.99–1.01; non-significant offsets (<0.2 m/s); and standard deviation errors of ~0.2 m/s.

Courtney *et al* [40] also reported on a comparison between these two LIDARs in 2008 and noted that, depending on the application, each had its strengths and weaknesses. For the focused (cw) system (ZephIR), the probe length, proportional to the square of the measuring height, is about 20 m at a measuring height of 100 m. For low heights, therefore, it is small but is quite large at heights over 150 m. The pulsed system (Windcube) has a constant probe length of a little less than 30 m (essentially determined by the transmitted pulse length). Therefore, for lower heights, the focused system was better suited whereas the pulsed system performed better at higher heights. Both systems performed well under most conditions in flat terrain. The authors suggested the ZephIR's cloud-correction algorithm (for the issue of backscatter from clouds, even when they are way outside the focal range) was deficient, but noted that they were assisting in the development of a more sophisticated version.

Marti *et al* [41] studied the use of LIDARs in complex terrain (Spain) and noted the usefulness of the technology compared to the installation of very tall masts in such locations, where access can often

be difficult. They adopted data quality control procedures and filtering criteria, noting the usefulness of parameters such as "points in fit" (in the case of the ZephIR).

With regards to offshore wind profiling, a ZephIR LIDAR, mounted on a platform at the Horns Rev wind farm in the North Sea, was successfully used to observe wind and turbulence characteristics [42]. Cup anemometer wind speed profiles (from three surrounding masts) were extended to 161 m above sea level with the LIDAR, and wakes from the wind farm were also observed.

Jaynes reported validation of a pulsed-laser LIDAR up to 100 m height in flat terrain (plains USA) and up to 80 m height in moderately complex terrain (France) [43]. Regression slopes (LIDAR *versus* mast) were close to 1 in both flat terrain and correlation coefficients >0.99 in both cases. LIDAR measured turbulence intensity at 16 m/sec was similar to that from the cup anemometers at each site—most notably it was within 1.4% at 80 m height in moderately complex terrain. However, poor LIDAR data coverage occurred at over 80m height in the latter instance, and the author surmised this was due to the presence of fog.

A pulsed-laser LIDAR was utilized, in both [44] and [45], at the sites of new generation 5MW wind turbines. In [44], the power curve of a 102 m hub height, 116 m rotor diameter turbine was measured, and the 0.67 Hz instrument sample rate was shown to be sufficient to resolve the short time dynamics of the power conversion process. In [45], the ambient wind field was measured before and after installation of a different 5MW model prototype, at a location near the north German coastline, in order to quantify the velocity deficits downstream from the turbine.

RS instrumentation for wind energy purposes has developed rapidly in the past few years, with ongoing changes being made to hardware and software elements. The (2009) performance (against cup anemometers) of the two types of LIDAR then available commercially (ZephIR and Windcube) was reported for flat terrain [46] and for complex terrain [47]. The former study reported extensive testing of the LIDARs at the Høvsøre Test Station in Denmark. Testing revealed significant weaknesses, which were being addressed by the manufacturers. The main problem with the ZephIR was the sensitivity to backscatter from clouds and mist, and the authors noted an improved cloud-correction algorithm had been implemented since their study. However, the problem of backscatter from low-lying mist remained unsolved. A further consequence of the Lorentzian weighting function (which also results in sensitivity to cloud backscatter) is the limitation in measuring altitude, due to an effective probe length which increases quadratically with range. The changes to the cloud-correction algorithm which were being made related to reducing the probe length, to address both these issues.

The study in [47] involved three LIDARs in complex terrain and results showed excellent linearity but also some deviations from the ideal slope. The data gathered was used in [48] to compare with numerically modelled flows (using the WASP Engineering software package) over complex terrain, which indicated a relationship between LIDAR errors and RIX (ruggedness index): Precise predictions for low RIX and correspondingly low precision for high RIX.

In flat terrain, LIDAR has proven to be precise in determining mean wind speeds and wind profiles. In complex terrain, however, the technique can lead to errors in horizontal wind speed of up to 10%. Computational fluid dynamics (CFD) modeling is now being employed as a means of correcting the observed bias in complex terrain [49]. In [50,51] CFD and LIDAR have also been applied together, in order to understand wind profile measurements from LIDAR better in complex and rough terrains.

1.3.3. Studies of LIDAR and SODAR Together

A number of intercomparison studies between LIDARs, SODARs and instrumented masts have been carried out, mostly located in flat, simple terrain on continental sites [52]. Calibration techniques were further developed for both techniques in the EU UpWind project [53].

Bradley and von Hünerbein compared all the new RS technologies for wind energy applications in 2007, and noted that the then current mono-static SODAR wind speed measurement accuracy was better than 1% compared to cup anemometers, particularly through improvements in reducing sensitivity to extraneous echoes and sound sources [37]. This study identified the main sources of error in SODAR measurements as incorrect estimation of the zenith angle of the acoustic beams; echoes from nearby fixed objects (e.g., masts); low SNR during times of poor temperature contrast; and echoes from rain.

In the same study, a number of limitations of the then relatively new ZephIR LIDAR were pointed out [37]: Although beam focusing reduced reflections from either side of the focal point, this did not eliminate them—contaminated data still remained if strong reflectors, such as clouds, were present, even at a much larger distance than the focal point (the 'cloud filter' had therefore been developed to filter these data); the effect of extended sensitivity around the focal point meant that spatial resolution along-beam was course at longer ranges; also, the relatively large conical scan used results in the three wind components being determined from spatially separated volumes of air (and because of this, reduced performance in complex terrain would be expected for LIDARs, as for mono-static SODARs). Despite this, the ZephIR showed good data availability and wind speed accuracies were approaching those achieved by SODARs. However, they concluded, both SODAR and LIDAR instruments still required field calibration against a mast.

Both LIDARs and SODARs have been tested offshore on fixed platforms at the sites of present or future offshore wind farms. The suitability of RS instruments operating over a long period in the marine environment (near the Nysted wind farm in the Baltic Sea) was assessed, in order to study the interaction of the wind farm with the ABL [54]. A number of shortcomings of each instrument were noted, such as the ambiguity of wind direction measurements from the (then prototype) ZephIR LIDAR and typical errors associated with the SODARs, such as height and tilt estimation errors due to changes in temperature, and level errors. However, they concluded that RS could be used to supplement met mast measurements for offshore applications.

Recent coordination of European LIDAR and SODAR research in the UpWind project has also led to a significant number of reports and studies in the remote sensing field published on-line [55], including studies on uncertainties, intercomparison methods, cloud correction in cw LIDAR, errors in turbulence measurement and errors in complex terrain.

1.4. Myres Hill Remote Sensing Project

The Myres Hill study was a joint industry project set up to test the capabilities of commercial LIDAR and SODAR systems for wind energy applications, in upland areas typical of many European sites being developed. It was the first such prolonged campaign in the UK or Ireland. The goals of the project were to compare these capabilities with the current wind energy industry standard for wind

measurements—the cup anemometer—and to explore any practical issues with deploying and operating these RS instruments in upland settings. The measurement campaign began in December 2007, with the installation of the instrumented mast, and the main intercomparison period (with all three systems operating) was from early February to mid-May 2008.

2. Experimental Method

2.1. Location

The study was undertaken at the NEL (National Engineering Laboratory) Myres Hill remote wind turbine test site, which is located about 8 km southwest of East Kilbride and about 20 km south of Glasgow, Scotland. The site has been in use for the testing of wind turbines and research and development since 1984.

The site has excellent exposure to the prevailing southwesterly winds. It is covered with grass and heather and has a low surface roughness, although large areas of forestry are within the vicinity of the summit of Myres Hill (Figure 1). At the time of the experiment, the 140-turbine Whitelaw wind farm was in the initial stages of construction about 2 km east of the site.

Figure 1. (a) Site layout plan; and **(b)** photograph of 80 m instrumented mast (view from northwest, with southeastern wind turbine, T2, in the background).

(a)   (b)
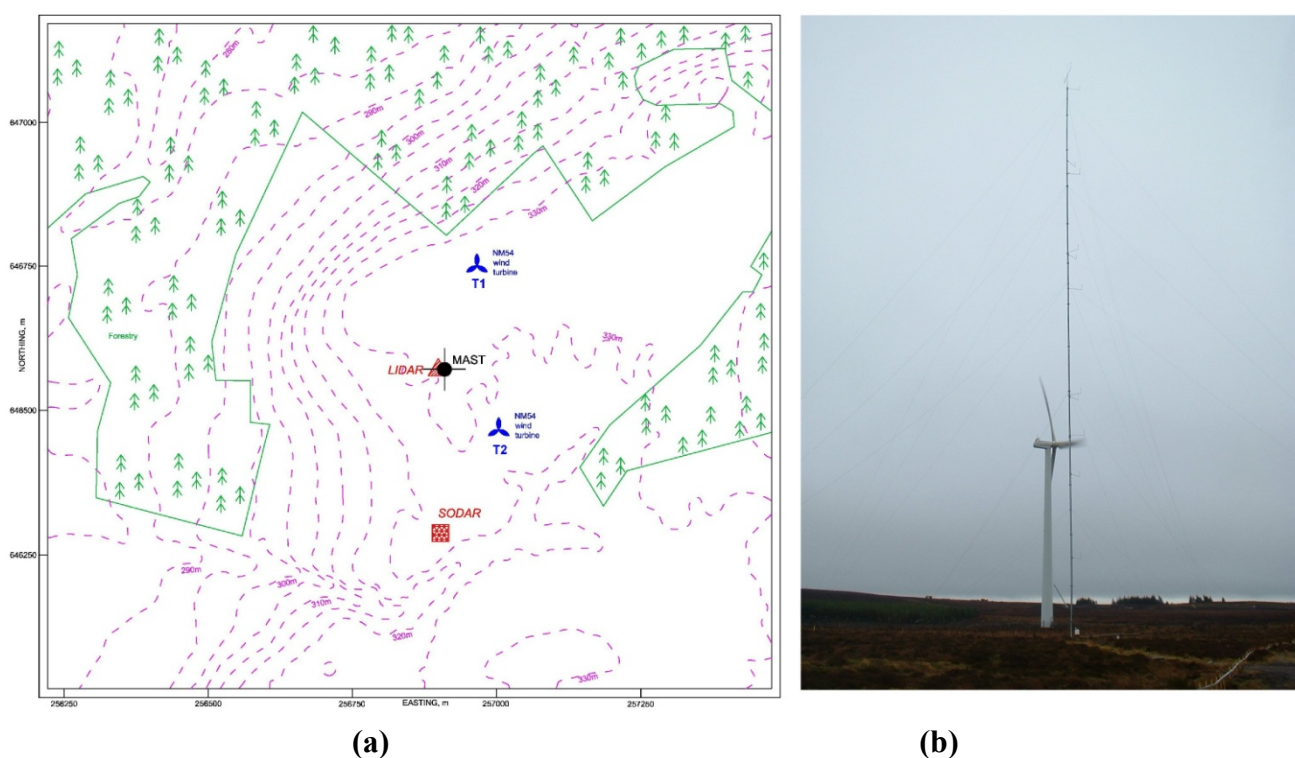
Figure 1 shows the orography of the site and surrounds, as well the major obstacles to wind flow: Two NEG Micon NM54 wind turbines (hub height 60 m, rotor diameter 54 m), located to the north-northeast and southeast of the site. Other, less important, obstacles on the site were two 50 m lattice wind monitoring masts and a number of small wind turbines on relatively short towers, as well as small buildings and huts.

2.2. Instrumented Meteorological Mast

An 80 m tilt-up mast was erected on the site for the experiment, in late December 2007. It was a tubular steel tower, with the bottom 60 m section constructed with outside diameter (OD) 219 mm tube, followed by a 17 m section of OD 193 mm tube and an OD75 mm top section of 2 m height. Two anemometers were mounted on the top of the mast at the same height (about 80 m above ground level), on a U-shaped boom and separated by a horizontal distance of 3.45 m. Details of these and the other relevant instruments mounted on the mast are given in Table 1. In addition to these, a Vaisala pressure sensor was also installed on the mast and a tipping bucket rain gauge approximately 8 m west of the mast.

Table 1. Monitoring mast instrumentation.

Reference	Instrument Type	Model	Height (m)	Orientation (°)
WS1	Cup Anemometer	Risø P2546A	80.35	306
WS2	Cup Anemometer	A100L2	80.35	126
WS3	Cup Anemometer	A100L2	65.00	182
US1	Ultrasonic Anemometer	Windmaster	63.00	180
WS4	Cup Anemometer	A100L2	50.30	270
WS5	Cup Anemometer	A100L2	50.05	182
WS6	Cup Anemometer	A100L2	30.25	266
WS7	Cup Anemometer	A100L2	30.00	182
WS8	Cup Anemometer	A100L2	20.00	183
WS9	Cup Anemometer	A100L2	10.00	183
WD1	Wind Vane	W200P	77.70	222
WD2	Wind Vane	W200P	45.00	221
WD3	Wind Vane	W200P	25.00	222
T1	Temperature Sensor	CS107	76.90	-
T2	Temperature Sensor	CS107	1.00	-

A Campbell Scientific CR1000 logger was used to log data. It was programmed to record, for every 10 minute period, mean, maximum, minimum and standard deviation of wind speed from each anemometer, mean and standard deviation of wind direction from each wind vane and the means of the other instruments (total bucket tips for the rain gauge). Data was gathered until early June 2008.

All anemometers were individually MEASNET (Measuring Network of Wind Energy Institutes) calibrated and mounted approximately 16 boom diameters above booms approximately 10 mast diameters long, consistent with the recommendations in [1].

2.3. LIDAR

The LIDAR employed was a ZephIR manufactured by QinetiQ (UK) and supplied from Natural Power (UK). LIDAR measurements were made at two locations, using two different units: Unit A was located approximately 12 m west of the mast for the duration of the measurement program, in order to be as close as possible to the mast. The potential of any significant blocking of the laser beam was

avoided by considering the 30° angle to the vertical through which the beam scans a cone. Cups, vanes and guy wires were all outside the scan disc in the upwind and downwind directions. Data was gathered from LIDAR Unit A from 5 February 2008 until 15 May 2008.

For the last month of the program, Unit B was co-located with, first, the Unit A LIDAR (as a check on the instrument's precision) and, following that, with the AQ500 Sodar (as a check between the instruments, given the separation of the SODAR and mast/LIDAR locations). Horizontal velocity at heights above ground level of 30 m, 50 m, 63 m, 80 m and 100 m were measured (measurements at 300 m are also performed as input for the ZephIR's internal cloud-correction algorithm). For every 10 minute period, the mean, max, min and variance of wind speed, and the mean of the wind direction were recorded for each of these heights. In addition, the LIDAR measured turbulence intensity, vertical velocity, temperature, humidity and pressure at each height. The internal quality control parameters 'Points in Fit' (PiF) and 'Packets in Average' (PiA), which are specific to the ZephIR LIDAR, were also recorded for every ten minute period. PiF refers to the number of radial wind speed measurements per scan, from which the instantaneous wind vector at the particular height is calculated. PiA is the number of instantaneous wind speed data in each ten-minute averaging period, at the particular height. These were used to filter the data when conducting correlations with the relevant mast-mounted cup anemometers.

The 'cloud correction' algorithm applied internally (to ameliorate over-prediction of wind speed by the ZephIR under dense cloud bases) was enabled in the LIDARs during the program. Although new algorithms for cloud correction became available during the study, for data consistency these were not applied. Wind direction data for a period in March and April was rejected due to malfunctioning of the on-board meteorological mast (which allows the LIDAR to determine which quadrant the wind is coming from).

2.4. SODAR

The SODAR employed was an AQ500 manufactured and supplied from AQ Systems (Sweden). It was initially installed about 80 m WSW of the planned mast location. However, following the observation of a fixed echo in the returns generated from the SODAR, following installation of the mast, the SODAR was moved to a location approximately 280 m south of the mast, prior to commencement of the study [53], see Figure 1. No echoes were observed in the data at this location. Data was gathered from the SODAR from 5 February 2008 until 15 May 2008.

Horizontal velocity at heights above ground level from 20 m up to 150 m, in increments of 5 m, were measured. For every 10 minute period, the mean and standard deviation of wind speed, and the mean of the wind direction were recorded for each of these heights. In addition, for every 10 minute period and at each of these heights, the SODAR measured the mean vertical velocity, the standard deviation of vertical velocity and the Signal-to-Noise ratio (SNR), the internal quality control parameter which has been used to filter the data when conducting correlations with the relevant mast-mounted cup anemometers.

3. Results and Discussion

3.1. Wind Data from Mast

3.1.1. Mast Data Quality

Data from the mast-mounted instruments was quality checked, and erroneous and suspect data flagged and not included in the following analyses. Data availability from the anemometers and wind direction sensors was very good (over 99.8% and 99.7%, respectively). Analysis of wind speed and temperature at the top of the mast indicated there were no icing events of any significant duration (*i.e.*, resolved by the 10 min averages logged).

Raw wind speed at 80 m (WS1) and wind direction from the top (78 m) direction sensor (WD1) are plotted in Figure 2 and indicate predominant wind components both in the southwest and northeast quadrants.

Figure 2. Wind speed and direction at top of mast during measurement period (unfiltered data).
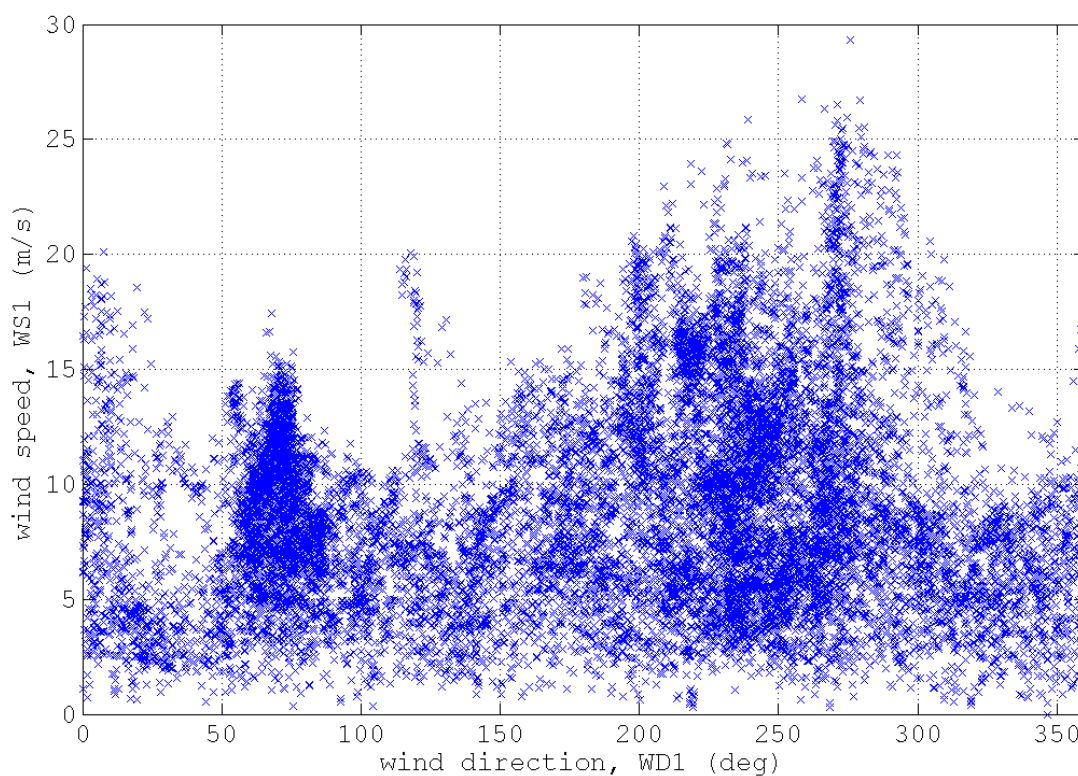

3.1.2. Direction Filtering

In order to exclude data from sectors affected by mast effects and upwind obstructions, predominantly the wakes from the two wind turbines, the guidelines in IEC standard 61400-12-1 were used [1]: The turbines have rotor diameters (D) of 54 m. The northern turbine was at a bearing of 17° from the mast, at a distance of 188 m, corresponding to 3.5D. At this distance, the disturbed sector to be excluded from the mast data, due to the wake of the wind turbine, is approx. 64°, corresponding to the sector 345–49° at the mast. The southern turbine was at a bearing of 138° from the mast, at a

distance of about 141 m (2.6D). The disturbed sector to be excluded from the mast data at this distance is approx. 73°, corresponding to the sector 101–175° at the mast. Between these two affected sectors, the sector 40–90° may also be influenced by mast effects, based on the orientation of the various instrument mounting booms in Table 1. Consequently, rounding the two wake influenced sectors outwards to the nearest 10° and excluding the remaining 90–100° sector, leaves the sector considered free from mast and wake effects to be 180–340°. The wake affected sectors for the LIDAR and SODAR are smaller than for the mast, as they are further away from, and in the prevailing wind sector of, the mast. The mast data within this wind direction range therefore provides the reference set for assessing the RS instruments.

### 3.1.3. Comparison between Cup Anemometers

Figure 3(a) is a comparison between the top mounted cup anemometers, which are from different manufacturers. Linear regression of the unfiltered data gives a slope of 0.996 and a correlation coefficient (R^2) of 1.000. The technique of mounting two anemometers at the same height, in the free stream above the mast, has become a standard arrangement for resource monitoring and is shown here to lead to high confidence in using data from either anemometer, as well as providing redundancy. However, each anemometer will affect the other for wind directions along the axis of the boom mounting the instruments. Therefore, a combination of the two anemometer measurements (when using the same model anemometer) for free stream wind directions, and only the upwind anemometer data for winds around a small arc along the mounting boom axis, will provide the most accurate wind speed measurements for resource assessments.

Figure 3. Mast instruments: Comparison between **(a)** 80 m top-mounted cup anemometers, and **(b)** wind vanes (78 m and 45 m). (February–May; 10 min averages).

(a)

(b)
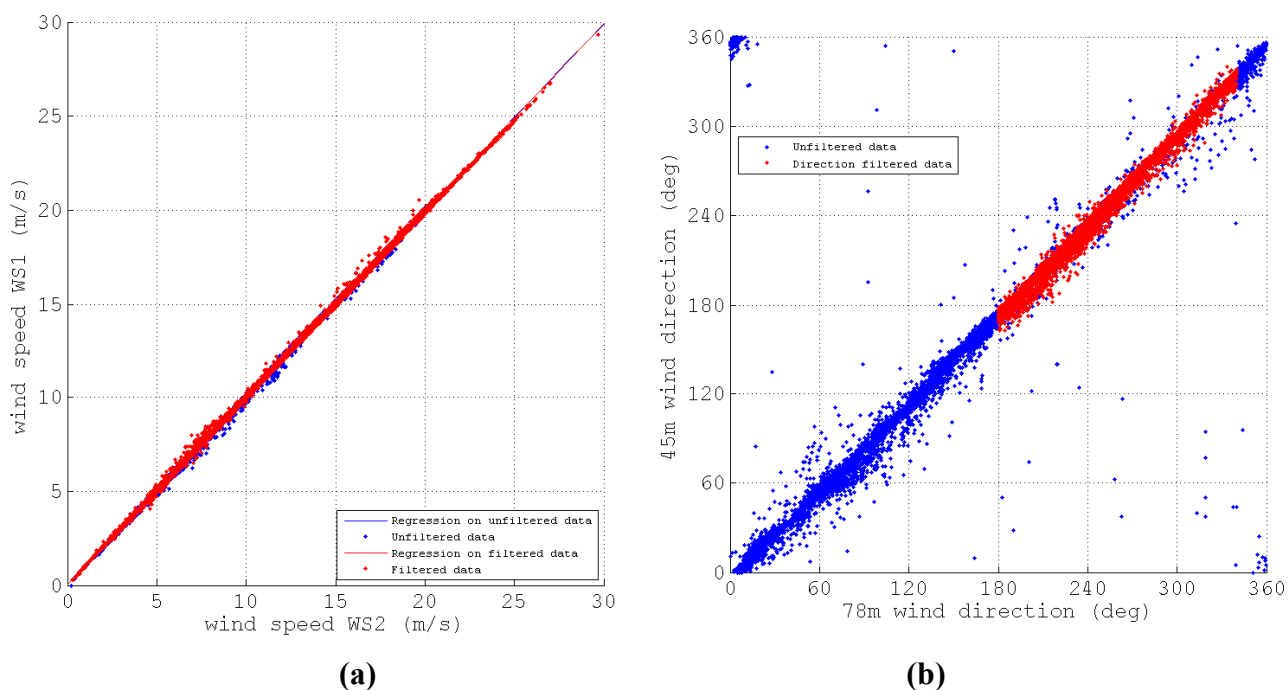
These effects are illustrated in Figure 4, which shows the ratio of the two top anemometer outputs as a function of wind direction, and reveals clearly the wind speed deficits recorded in each anemometer at the azimuths of their respective mounting booms: 126° and 306°. Another less pronounced effect on the anemometers occurs at about 20°, which is the approximate direction of the northern turbine (T1) from the mast. However, the effects on the anemometers differ, in that WS2 is in deficit at slightly lower azimuths than WS1, and the deficit on WS1 is more pronounced. Although the turbine is almost 190 m from the mast at this point, these effects are likely due to the relatively large horizontal separation of the anemometers (3.45 m) and the orientation of their mounting plane, which is approximately perpendicular to T1.

Figure 4. Directional variation in ratio of 80 m top-mounted anemometer wind speeds. (February–May; 10 min averages).
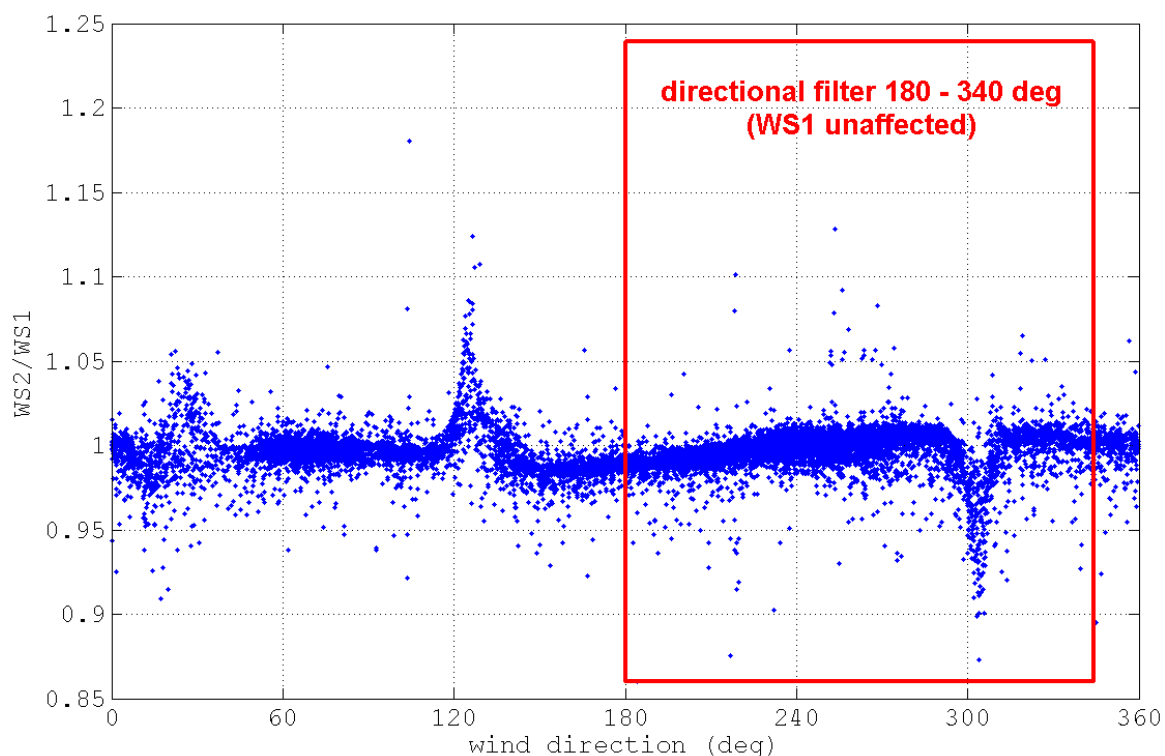
The effects of the southern turbine (T2, expected at wind directions around 138°) cannot be distinguished in the data from top-mounted anemometers in Figure 4, even though this turbine was closer to the mast than T1. It is possible that, because the direction to T2 is close to that of the axis of the WS2 cross-boom (126°), the velocity deficits from the turbine wake recorded at both WS1 and WS2 are similar and mask the effect of anemometer WS2 on anemometer WS1. However, analysis of data from the 50 m and 65 m anemometers show obvious wind speed deficits at around 138°, the direction to the T2, suggesting that the turbine wake may be mostly constrained to below the 80 m height level.

The turbine wakes, and the effect of each anemometer on the other, result in most of the significant scatter illustrated in Figure 3(a). These effects are mostly removed through the directional filtering applied, which is illustrated by the red box in Figure 4. Note, the dip in WS2/WS1 at ~306° corresponds to the deficit at WS2 caused by the wake of WS1, and not as a speed up in the latter. This

deficit in WS2 is also visible in the direction filtered data of Figure 3(a), as the distinct outliers above the line of slope = 1 (mostly between 5 and 20 m/s). Therefore, the use of WS1, along with the direction filtering outlined, provides the least affected cup anemometer data and the reference for the 80 m level in the comparisons with the RS data following.

Similar analyses of data from all the anemometers below 80 m, mounted on booms facing approx. south, clearly indicate the shadow effects of the mast at wind directions approximately 20° either side of north. Again, these effects are removed with the directional filtering applied. The wind shear exponent (α), a characteristic of the site, calculated using the raw 80 m and 30 m cup anemometer data (WS2 and WS7), was 0.19. Using the direction filtering described above, and ignoring data with 80 m wind speed below 3 m/s, gives an α of 0.20. Variation in the wind shear exponent is discussed in the Appendix.

3.1.4. Comparison between Wind Vanes

Comparison of the 78 m and 45 m wind directions is presented in Figure 3b, for the raw and direction-filtered data, indicating good agreement, with a slope of 1.018 and an R^2 of 0.995 for the direction filtered data. However, the offset of this regression line is −11.4°, suggesting a misalignment in one of the vanes. This was likely to be the lower one (45 m), as the agreement between both RS instruments' wind directions at 80 m and the 78 m wind vane are both good (see Section 3.4).

Analysis of the differences between the top two wind vane outputs against wind direction does not reveal any tower effects in the data, presumably as the boom orientation of each wind vane is the same. Comparison of the vane differences against wind speed indicates most scatter is at very low wind speeds, as expected.

3.1.5. Meteorological Conditions during Study

Meteorological conditions during the study were typical for the time of year. Temperatures ranged from −4 °C to +21 °C (with a mean of 5 °C); pressure varied from 922 to 1,003 hPa; and the maximum rainfall recorded was 2 mm in 10 minutes. Temperature, rainfall and wind shear data, from the mast; and aviation METARS (Meteorological Aviation Routine Weather Report) data, from Glasgow Airport (as potential proxy data for the occurrence of clouds and other precipitation types not recorded on site), are further discussed in the Appendix.

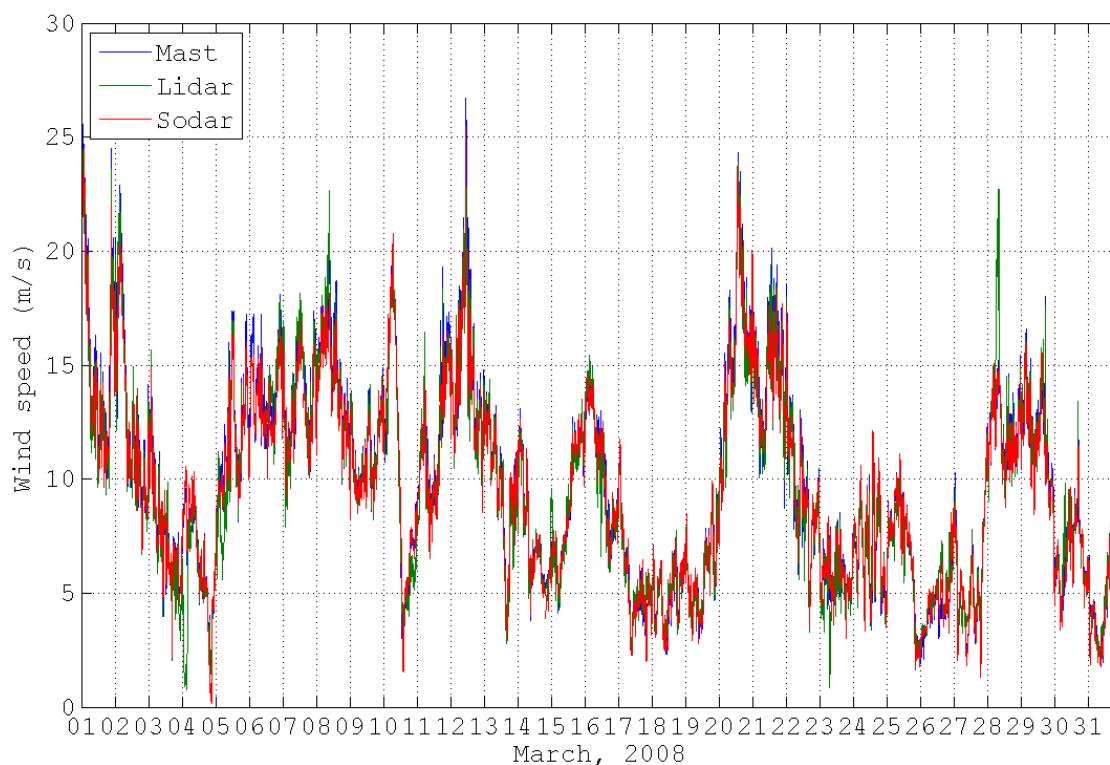### *3.2. RS Wind Speed Data*

3.2.1. Raw Data

There is general agreement between the cup anemometer wind speeds and the wind speeds recorded by the SODAR and LIDAR. See, for example, the monthly plot of unfiltered 80 m wind speed data for March in Figure 5. However, there are frequent periods during which both RS systems tend to under-record wind speed compared to the cup anemometer. In addition, there are also periods when the LIDAR has reported both significantly higher and lower wind speeds compared to both cup and SODAR.

3.2.2. Data Filtering

Filtering of the raw 10-min average data was carried out in order to remove effects caused by turbine and mast wakes, poorer quality data and low wind speeds:

1. Direction filtering, as described in Section 3.1.2.
2. Data quality filtering, based on the parameters 'Points in Fit' (PiF) and 'Packets in Average' (PiA) for the LIDAR and Signal-to-Noise (SNR) ratio for the SODAR. These internal quality control parameters are indicators of the number of data points during an averaging interval available for internal processing in the RS instruments, with smaller values indicating poorer quality averages. As no guidance on 'external' processing is provided by the instrument manufacturers, the optimum levels for filtering were calculated empirically, with the aim of maximizing the number of data available for the intercomparison exercise and regression calculations, while eliminating as many poor quality data points as possible. For the LIDAR, filtering was carried out such that only data with PiF ≥ 80 and PiA ≥ 24 were used, while for the SODAR, only data with SNR ≥ 50 were used.
3. For the wind speed comparisons, further filtering was carried out such that only data where the corresponding cup anemometer was ≥ 3 m/s were used, eliminating low wind speed periods during which most large wind turbines are not generating. This filtering is also important as the measurement uncertainty in cup anemometers for wind energy applications is usually higher at wind speeds below 4 m/s (below which the standard classification for cup anemometers is not defined in [1]). Note, for the direct LIDAR-SODAR comparison (Section 3.3.2), filtered data refers to periods when *both* RS instruments have recorded ≥ 3 m/s.

Figure 5. Comparison of 80 m wind speeds from cup anemometer (Mast), LIDAR and SODAR. (Raw, *unfiltered* data; 10 min averages).

3.3. Wind Speed Regression Analysis

3.3.1. RS and Mast Data Comparisons

For each of the four study heights, unfiltered and filtered data from each RS instrument were linearly regressed against the relevant cup anemometer data. Figure 6 illustrates these correlations for the LIDAR and SODAR, along with the least-squares lines of best fit, for the 80 m level. The counts of filtered data points compared to unfiltered data in these plots are (a) 7622/14324 (LIDAR) and (b) 7234/14405 (SODAR). A summary of the linear regression results for all four study heights is given in Table 2, and indicates generally good agreement between the RS instruments and the relevant height cup anemometer (as the de facto standard).

Figure 6. Comparison of 80 m wind speeds with WS1 cup anemometer (Mast): **(a)** LIDAR and cup; and **(b)** SODAR and cup, (February–May; 10 min averages).
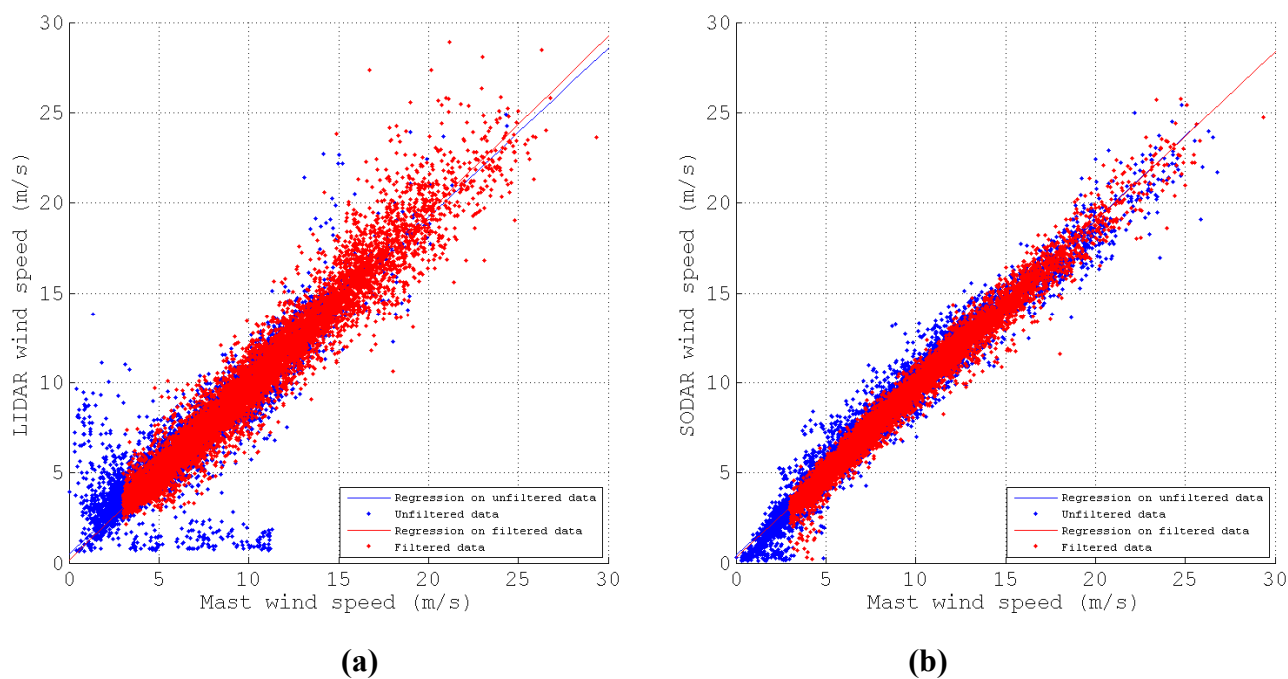

(a)

(b)

Table 2. Regression Results for Wind Speed Comparisons.

RS instrument	Study height	Slope	Offset	R^2
LIDAR	30 m	0.967	0.38	0.972
	50 m	0.973	0.33	0.973
	63 m [1]	0.967	0.27	0.971
	80 m	0.969	0.17	0.970
SODAR	30 m	0.944	0.30	0.976
	50 m	0.937	0.37	0.988
	65 m	0.933	0.37	0.989
	80 m	0.936	0.30	0.989

[1] 63 m LIDAR and 65 m mast cup anemometer.

The regression line for the unfiltered LIDAR data, with a slope of 0.937 and offset 0.47 ($R^2 = 0.955$), was significantly different to the filtered results, as is evident in Figure 6(a). Conversely, the much lower scatter in the SODAR data (Figure 6(b)), particularly at higher wind speeds, resulted in a similar regression to the filtered data: slope 0.932 and offset 0.42 ($R^2 = 0.986$).

Filtering for obstacle and mast effects reduced the scatter in the comparison plots, but does not remove all scatter nor explain some of the trends observed in the plots.

The comparison plots show that scatter in both RS instruments was greater for wind speeds generally below about 6–7 m/s and above 15 m/s. In particular, the LIDAR data exhibited greater scatter at wind speeds >15 m/s at 80 m, whereas the greatest scatter in the SODAR data at this height was for wind speeds below 5 m/s.

The LIDAR-Cup and SODAR-Cup wind speed residuals were plotted against cup wind speed and wind direction (see Figure 7(a,b)), in order to investigate these differences. Figure 7(a) shows that the LIDAR records high at decreasing wind speeds and there are some periods when the LIDAR is close to zero for (cup) wind speeds up to 10 m/s. Most of these anomalous data do not appear when the filters are applied. For the SODAR (Figure 7(b)), lower wind speeds are occasionally recorded at both low and high cup wind speeds. Similar to the LIDAR, there are also periods when the SODAR wind speed is very low (approaching zero), up to wind speeds of about 5 m/s, particularly at heights above 50 m. Filtering removes some of these low wind speed outliers in the SODAR data, but not all (see Figure 7(b)). It is noted that measurements from cup anemometers for wind speeds below about 4 m/s are much more uncertain and their output tends to be non-linear in this range.

The relationships between these wind speed residuals and wind direction (Figure 7(c,d)) reflects, to a degree less prominent than when comparing the top anemometers, the anemometer and turbine wake effects. The cluster of −10 m/s LIDAR-Cup differences at ~80° indicates the wake of the mast has actually affected the LIDAR laser beam for roughly easterly winds. The LIDAR-Cup residuals also exhibit considerable scatter in the "free stream" of 180–340°. For the Sodar-Cup differences, this free-stream scatter is not as pronounced.

The greater scatter in the LIDAR data may be related to the method with which the instrument corrected for clouds. A new cloud correction algorithm from the OEM became available during the course of the measurement programme, but was not installed in the LIDAR due the possibility of introducing inconsistency into the LIDAR data. Recent work on cloud effect removal [56] suggests a strategy of running the LIDAR at an additional greater height of typically 800 m, which is greater than that used in this study (300 m). Qualitative cloud records from Glasgow Airport (aviation METARS data) did not correlate well with the site data, probably due to the significant separation distance from the airport to the site.

Similarly, the airport data on mist and fog also did not correlate well with periods of scatter in the LIDAR. However, in this case, the presence of mist and fog has been inferred from relative humidity (RH, calculated at each measurement height by the LIDAR) and temperature (from the mast sensors): The LIDAR and cup data for 80 m were filtered for data with RH (80 m) ≥ 90% *and* T (77 m) ≤ 1 °C (conditions relevant for the formation of mist at the time of year the measurements were made). This resulted in the rejection of only 403 records out of 14.324, and very little change to the regression between LIDAR and Cup anemometer. Only on-site measurements of mist and fog may therefore provide better understanding of uncertainty in LIDAR data caused by such conditions. It has been

noted in the literature [56] that high wind shear can increase the risk of overestimation of wind speed in cw LIDARs. Analysis of the LIDAR-Cup wind speed residuals and the wind shear exponent, α, indicated that such effects were not significant during this study, even though numerous high wind shear events occurred. This analysis is included in the Appendix.

Figure 7. LIDAR-Cup **(a,c)** and SODAR-Cup **(b,d)** wind speed differences, as a function of wind speed **(a,b)** and direction **(c,d)**; *Filtered by direction and data quality parameter only.* (February–May; 10 min averages).
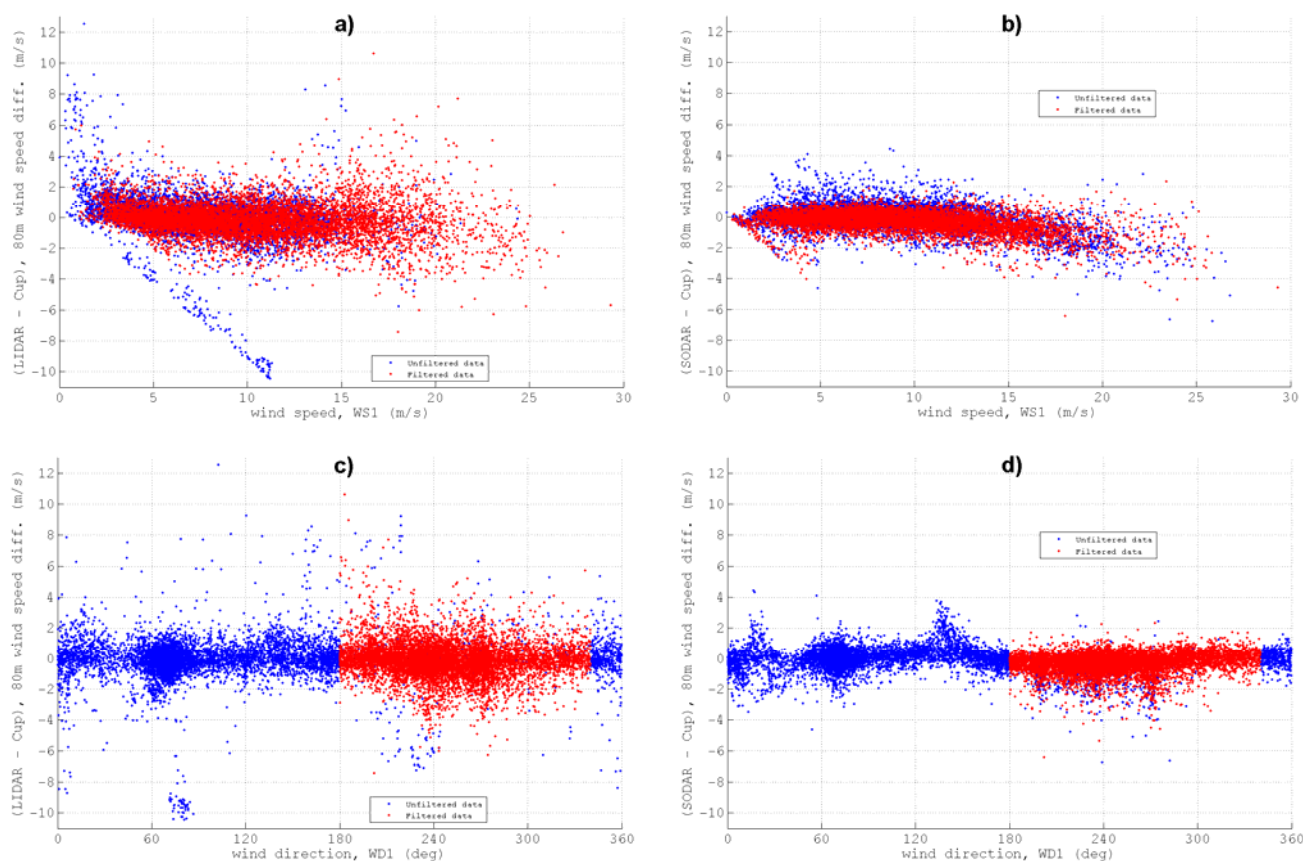

Effects of rain on LIDAR measurements of wind speed or the parameters PiF and PiA did not appear significant, see Figure 8(a,c), which agrees with [56].

Analysis of the LIDAR-Cup wind speed residuals against PiF and PiA, however, shows clearly the importance of filtering based on these internal data quality parameters, although the LIDAR values can be at times lower than the Cup values (e.g., February) or higher (e.g., May data).

Heavy rain events appear to reduce data quality in the SODAR and lead to lower measured wind speed, as shown in (Figure 8(b,d)). These results are similar to those in [23], where higher wind speed standard deviations were reported during rain, and also agree with the findings in [37].

Interestingly, at the 80 m level and for both the LIDAR and SODAR data, the scatter was reduced in the wind speed range from about 7 to 15 m/s. This is generally the steepest part of a wind turbine power curve and hence the most difficult range in which to forecast wind power [57], suggesting RS techniques would be useful in providing accurate real-time data for input to wind power forecasting models.

Figure 8. (a) LIDAR-Cup and **(b)** SODAR-Cup wind speed differences and rain; and internal quality parameters and rain: **(c)** LIDAR (PiF and PiA) and **(d)** SODAR (SNR). (Unfiltered; March data only; 10 min averages).
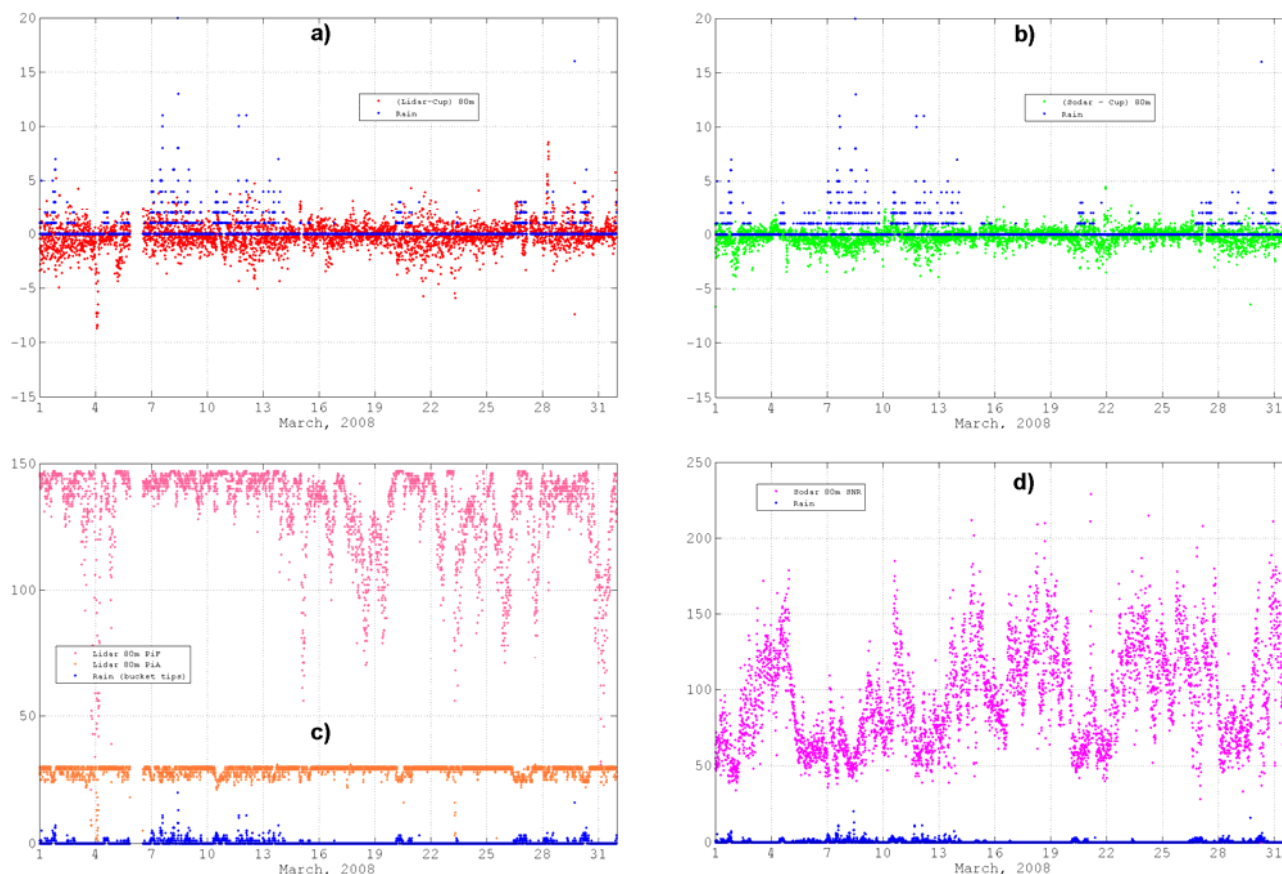
Given the moderately complex terrain of the site and its surroundings (orography as well as substantial forested areas), it is likely that the large separation (280 m) between the SODAR and the mast is the reason for the generally lower wind speeds recorded by the SODAR. At 30 m measurement height, a greater scatter was observed in the SODAR data and this may also be in part due to these terrain effects, in particular increased turbulence due to local forestry.

Further study is needed comparing wind speeds at greater measurement heights, which was limited in this study to 80 m (the height of the mast).

Note, this discussion applies only to the SODAR and LIDAR models and the instrument software configurations provided, as well as only to the Myres Hill site and the locations of all the instrumentation on-site. It is particularly noted that the instruments and the RS techniques underpinning them are constantly evolving. The results here are therefore a 'snapshot' in time with regards to the development of these RS methods.

3.3.2. LIDAR-SODAR Comparison above Mast Height

Data at 100 m from both RS systems was also compared, to investigate the use of RS in determining wind speed above the height of typical (*i.e.*, lower cost) monitoring mast heights. Figure 9 shows the greater spread in recorded values from each system, compared to the comparison plots

against the mast cup anemometers above. (Note, low wind speed filtering was carried out by rejecting data where either LIDAR or SODAR wind speeds were below 3 m/s.) Slope and offset of the data (unfiltered results in brackets) were 0.988 (0.963) and 0.14 (0.34) respectively, and the correlation coefficient was 0.962 (0.946), suggesting a good agreement between the two methods, although it is noted that both systems recorded wind, on average, lower than the cup anemometer standard.

Figure 9. Comparison of 100 m **(a)** wind speed; and **(b)** wind direction, from LIDAR and SODAR. (February–May; 10 min averages).

(a)   **(b)**
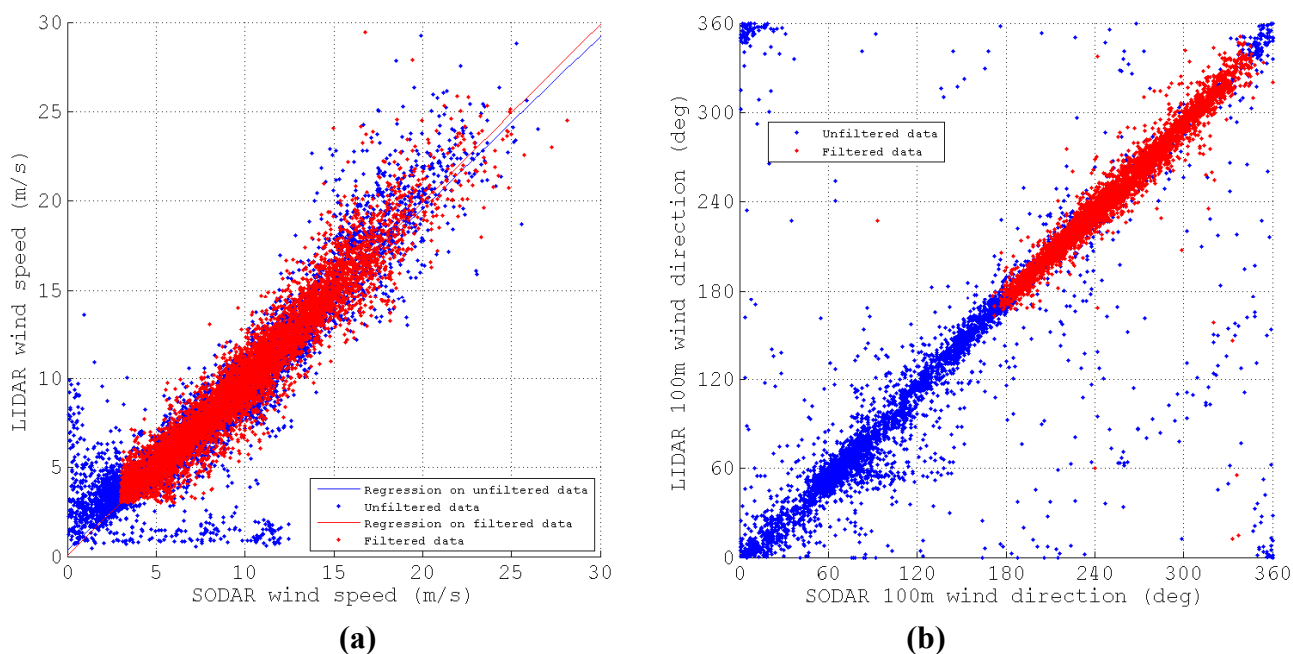
3.4. Wind Direction Regression Analysis

Figure 10(a,b) shows the regression plots for wind direction data at 80 m and Table 3 lists the regression results. Good agreement between the RS instruments and the mast-mounted wind vane (as the de facto wind direction measuring standard) is observed. However, as with the wind speed, the LIDAR produces wind directions closer to that of the wind vane, but with greater scatter. It is noted that there were less LIDAR data points for the wind direction regression analysis due to the inoperability of the on-board meteorological mast (as detailed in Section 2.3). In addition, some outliers in the LIDAR wind direction data are in a band approximately 180 degrees out of phase with the mast wind data, indicating the LIDAR did not always detect the correct hemisphere from which the wind is coming, even with the on-board met mast operable. The counts of filtered data points compared to unfiltered data in these plots are (a) 5372/9693 (LIDAR) and (b) 7234/14435 (SODAR).The comparison between LIDAR and SODAR wind directions at 100 m are shown in Figure 9(b) and the results of the regression analysis on these data are also provided in Table 3.

Figure 10. Comparisons of wind direction from **(a)** LIDAR (80 m) and Mast (78 m); and **(b)** SODAR (80 m) and Mast (78 m). (February–May; 10 min averages).
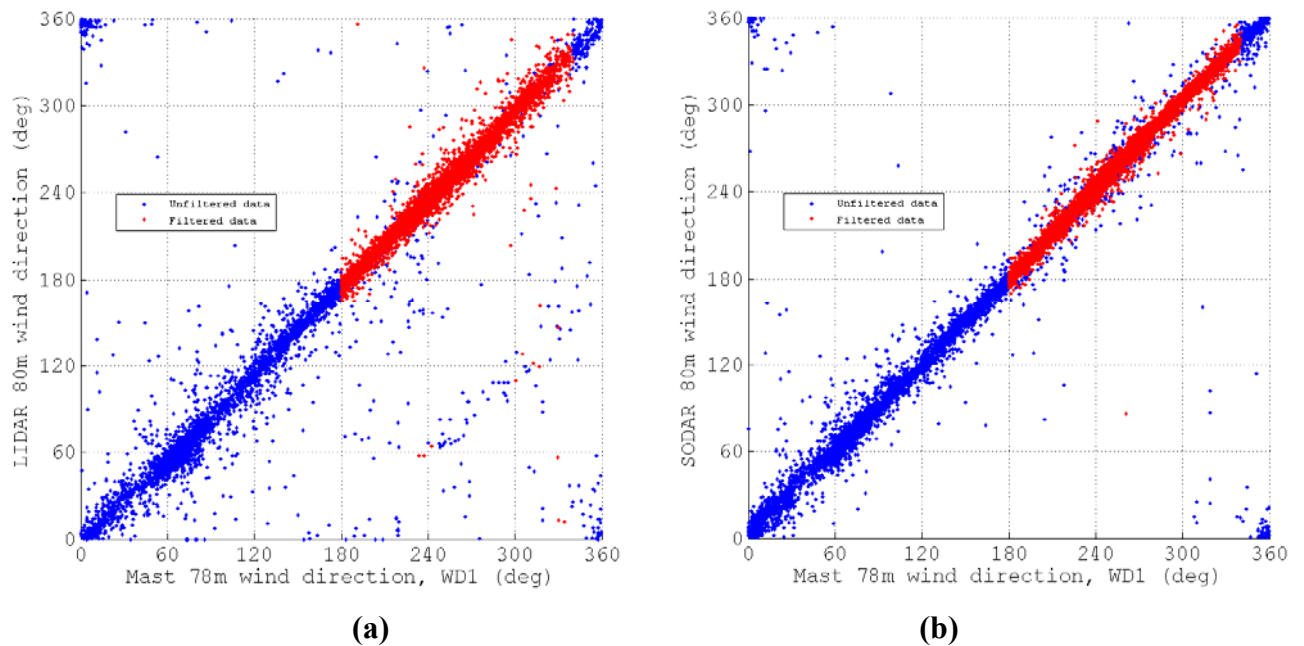

(a)   (b)

Table 3. Regression Results for Wind Direction Comparisons.

	Slope	*Offset*	R^2
LIDAR 80 m and Mast [1]	0.982	−1.2	0.947
SODAR 80 m and Mast [1]	1.022	−3.2	0.993
LIDAR 100 m and SODAR 100 m	0.950	5.0	0.953

[1] Compared with 78 m mast wind vane.

*3.5. Wind Speed Standard Deviation and Turbulence Intensity Comparisons*

Turbulence intensity (TI) is a key parameter in wind energy resource assessment. TI for wind energy applications is defined by σ/v_{av}, where σ is the standard deviation of the 10 minute average wind speed, v_{av}.

The correlation coefficients that result from plotting the TI from the LIDAR and SODAR data against the cup anemometer-derived TI are 0.31 and 0.59 respectively, indicated a poor ability of both these RS instruments to measure this parameter during the study. However, plotting only the standard deviations of the wind speed measurements (Figure 11) reveals much better agreement, in particular with the LIDAR data: The correlation coefficients increase to 0.83 and 0.86 for the LIDAR and SODAR respectively.

The regression line characteristics for the filtered standard deviation data are: (a) 0.86 [slope], −0.08 [offset] (LIDAR); and (b) 0.95 [slope], −0.10 [offset] (SODAR).

Generally better measurements of TI have been observed in other RS studies (e.g., [31]), however, these have been in generally flatter terrain and with different instruments (e.g., the Triton SODAR).

Figure 11. Standard deviation of 80 m wind speed: (**a**) LIDAR, (**b**) SODAR. (February–May; 10 min averages).
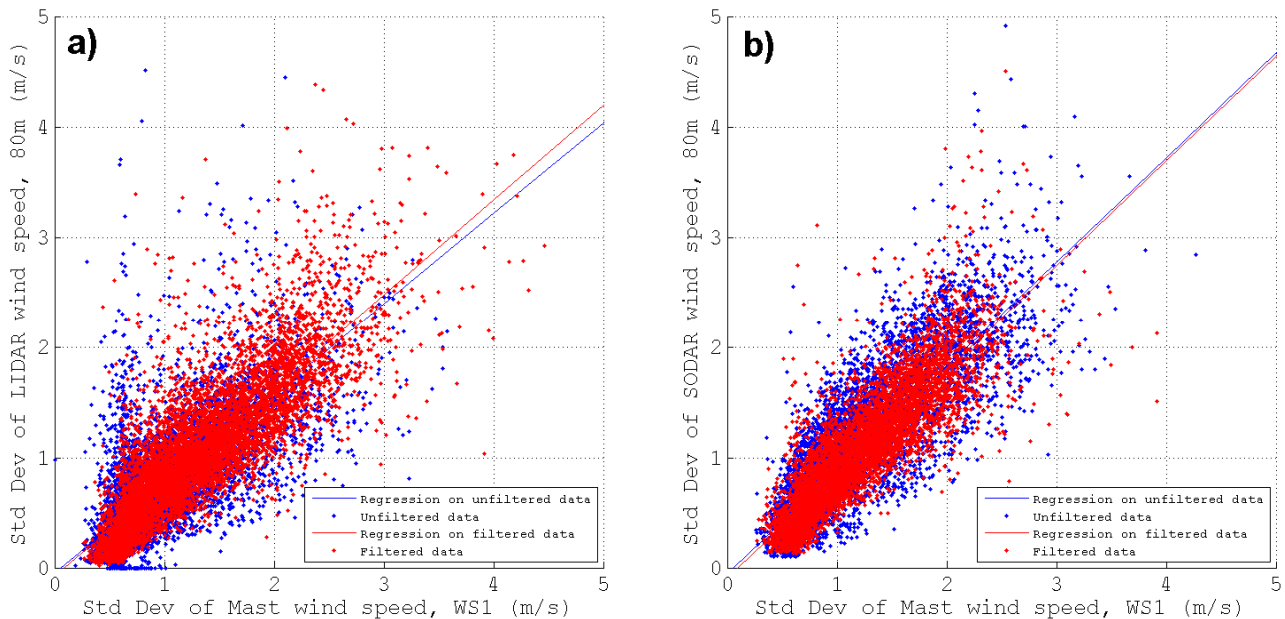
3.6. Results of Co-location of RS Instruments

When the second ZephIR LIDAR (Unit B) was co-located beside the mast for 2 weeks (with all system settings identical to the first), an excellent agreement between the two LIDARs was observed: For both wind speed and direction, the regression slope was generally better than 0.99 and $R^2 > 0.999$. This lent confidence to the LIDAR measurements from the first unit (A).

The re-location of LIDAR unit B to a site adjacent to the SODAR unit, late in the measurement program, was to perform a *de facto* site calibration to the SODAR data in an attempt to correct for terrain effects caused by the large separation of Mast and SODAR. However, it appears to have been too short a period to carry out a rigorous statistical analysis.

4. Summary and Conclusions

Detailed knowledge of the wind resource is essential for wind farm development, in the exploratory, financing and operational phases. Mast-mounted cup anemometry has been the de facto standard for most of the modern history of wind energy. However, the use of ever increasing mast heights to keep up with wind turbine hub heights has necessitated development of new techniques, in particular those for measuring the wind remotely. Doppler effect techniques such as LIDAR and SODAR, utilizing, respectively, light and sound transmission and reception from instruments located at ground level, have increasingly been applied to the field with increasing success. Commercial instruments are now being deployed worldwide.

These remote sensing (RS) techniques, however, measure the wind field over a much larger volume than that of a cup anemometer. Many studies of these methods have taken place in flat terrain, and therefore this study set out to investigate LIDAR and SODAR wind measurements in upland terrain more typical of the areas where much of the modern wind turbine fleet is now being installed in

Europe and indeed around the world. With current uncertainty in the accuracy and precision of wind measurements using RS, particularly in terrain that is not flat, further development of the instrumentation and data processing methods is an important step in increasing the confidence in RS techniques.

An intercomparison of LIDAR, SODAR and mast-mounted cup anemometer wind measurements has been carried out at an upland site with moderately complex terrain in Scotland. Correlations between the various instruments have been made, at a number of heights ranging from 30 m up to 100 m above ground level. A good level of correlation was observed in most cases, although the raw data indicated a number of errors in the RS measurements (using the cup anemometers as the standard), and typically both RS methods recorded lower wind speeds than the cup anemometers.

Filtering for mast and obstacle wakes, low wind speeds and internal instrument parameters (reflective of the quality and quantity of data available during each 10 minute averaging period), decreased the scatter in each comparison and increased the positive correlation. The LIDAR-Cup regression slopes were approximately 0.97, which compare well with slopes of better than 0.99 in similar studies carried out in flat terrain. For the SODAR-Cup regressions, the slopes were approximately 0.94, compared to slopes of better than 0.98 in similar studies carried out in flat terrain. The SODAR data had a lower scatter and hence higher correlation coefficient (~0.99), compared to that of the LIDAR (~0.97). It is therefore considered that the LIDAR was more accurate and the SODAR more precise in measurements of wind speed during this study.

The SODAR wind speeds measured were generally lower during rain events. However, increased scatter in the LIDAR data during rain events did not appear significant.

The greater scatter in the LIDAR data may be related to the method with which the instrument corrected for clouds. Although a new cloud correction algorithm became available during the course of the measurement program, it was not installed, in order to maintain consistency in the LIDAR data. Qualitative cloud information obtained from Glasgow Airport METARS data did not provide any insight into these issues, probably due to the large distance between the Myres Hill study site and Glasgow Airport.

The possibility of low lying cloud or fog/mist episodes could not be ruled out, as there was no on-site recording of them and the Glasgow Airport METARS data on these events was (similar to the METARS cloud data) inadequate. However, the inference of these episodes using site temperature measurements and LIDAR relative humidity measurements suggested such conditions were rare and may not explain any significant scatter in the LIDAR data.

The potential for high wind shear to increase the risk of overestimation of wind speed in cw LIDARs was also analysed and found to be insignificant during the study.

It is likely that some of the SODAR variations are due to the local terrain, as the instrument was located 280 m from the mast in semi-complex terrain (and at a lower altitude). Although the LIDAR was located adjacent to the mast, such terrain effects may also be the cause of some scatter in the LIDAR data.

At the 80 m level in both the LIDAR and SODAR data, a lower scatter was observed in the approximate wind speed range 7–15 m/s. This is generally the steepest part of a wind turbine power curve and hence the most difficult range in which to forecast wind power, suggesting RS techniques could be useful in providing accurate real-time data for input to wind power forecasting models.

Although turbulence intensity measurements by both RS methods were poorly correlated with the standard cup anemometer measurements, the correlations between the standard deviations of the wind speed measurements were reasonable, particularly that of the SODAR. Further work is necessary to enable accurate measurement of turbulence directly using these techniques, as, the parameter is particularly important for site classification and turbine selection.

Finally, LIDAR and SODAR are of particular interest in upland terrain, due to the difficulty in constructing masts there and also because the wind resource tends to be highly variable at different locations around wind farm sites. It is very cost prohibitive to construct many masts at different locations in order to characterize the wind resource. However, it may be relatively easy to position RS equipment at many locations within a site and the cost savings could be substantial.

Acknowledgements

References

1. International Electrotechnical Commission (IEC). *IEC 61400-12-1 Ed.1: Wind Turbines: Part 12-1: Power Performance Measurements of Electricity Producing Wind Turbines*; IEC: Geneva, Switzerland, 2007; pp. 67-74.
2. Pedersen, T.F. *Development of a Classification System for Cup Anemometers—CLASSCUP*; Risø-R-1348(EN); Risø National Laboratory for Sustainable Energy, Technical University of Denmark: Roskilde, Denmark, 2003.
3. Lackner, M.A.; Rogers, A.L.; Manwell, J.F. *Wind Energy Site Assessment and Uncertainty*; Renewable Energy Research Laboratory, University of Massachusetts: Amherst, MA, USA, 2006.
4. Bradley, S. *Atmospheric Acoustic Remote Sensing*; CRC Press: Boca Raton, FL, USA, 2008.
5. Thomson, D.W.; Coulter, R.L. Analysis and simulation of phase coherent ACDAR sounding measurements. *J. Geophys. Res.* **1974**, *79*, 5541-5549.
6. Little, G.C. Acoustic methods for the remote probing of the lower atmosphere. *Proc. IEEE* **1969**, *57*, 571-578.
7. Graber, W.K. SODAR monitoring of the atmosphere—Recent developments. *Appl. Phys. B* **1993**, *57*, 1-2.
8. Vogt, S.; Thomas, P. SODAR—A useful remote sounder to measure wind and turbulence. *J. Wind Eng. Ind. Aerodyn.* **1995**, *54-55*, 163-172.
9. Crescenti, G.H. The degradation of Doppler SODAR performance due to noise: A review. *Atmos. Environ.* **1998**, *32*, 1499-1509.
10. Carsewell, A.I. LIDAR measurements of the atmosphere. *Can. J. Phys.* **1982**, *61*, 378-393.
11. Argall, P.S.; Sica, R.J. LIDAR. In *Encyclopedia of Imaging Science and Technology*; Hornak, J.P., Ed.; John Wiley & Sons: New York, NY, USA, 2002.
12. Wandinger, U. Introduction to Lidar. In *Lidar: Range-Resolved Optical Remote Sensing of the Atmosphere*; Weitkamp, C., Ed.; Springer: New York, NY, USA, 2005; pp. 6-11.

13. Menut, L.; Flamant, C.; Pelon, J.; Flamant, P.H. Urban boundary layer height determination from lidar measurements over the Paris area. *Appl. Opt.* **1999**, *38*, 945-954.

14. Murayama, T.; Okamoto, H.; Kaneyasu, N.; Kamataki, H.; Miura, K. Application of lidar depolarization measurement in the atmospheric boundary layer: Effects of dust and sea-salt particles. *J. Geophys. Res.* **1999**, *104*, 31781-31792.

15. Buttler, W.T.; Soriano, C.; Baldasano, J.M.; Nickel, G.H. Remote sensing of three-dimensional winds with elastic lidar: Explanation of maximum cross-correlation method. *Bound.-Lay. Meteor.* **2001**, *101*, 305-328.

16. Stephens, G.L. *Remote Sensing of the Lower Troposphere: An Introduction*; Oxford University Press: New York, NY, USA, 1994; p. 427.

17. Högström, U.; Asimakopoulos, D.N.; Kambezidis, H.; Helmis, C.G.; Smedman, A. A field study of the wake behind a 2 MW wind turbine. *Atmos. Environ.* **1988**, *22*, 803-820.

18. Beyrich, F.; Klug, H.; Schomburg, A.; Kalass, D.; Weisensee, U.; Albers, A. Measurement of the Wind and Turbulence Fields in the JADE Wind Park with SODAR. In *Proceedings of the EWEA European Wind Energy Conference*, Thessalonica, Greece, 10–14 October 1994.

19. Dam, J.J.D.; Werkhoven, E.J. *Mini-SODAR for Wind Energy Application: Explorative Experimentation*; Report ECN-C--99-034; Energy Research Centre (ECN): Petten, The Netherlands, 1999.

20. Antoniou, I.; Jørgensen, H.E.; Petersen, S.M. Remote Sensing of the Wind Speed for Wind Energy Purposes Using a SODAR. In *Proceedings of the EWEA European Wind Energy Conference*, Copenhagen, Denmark, 2–6 July 2001.

21. Hayashi, T.; Liu, W.; Sassa, K. A preliminary investigation of low-cost SODAR anemometry. *Wind Eng.* **2003**, *27*, 285-297.

22. Folkerts, L.; Barthelmie, R.; Sanderhoff, P.; Ormel, F.; Eecen, P.; Stobbe, O. SODAR wind velocity measurements of offshore turbine wakes. *Wind Eng.* **2001**, *25*, 301-306.

23. Barthelmie, R.; Folkerts, L.; Ormel, F.; Sanderhoff, P.; Eecen, P.; Stobbe, O.; Nielsen, N. Offshore wind turbine wakes measured by SODAR. *J. Atmos. Ocean. Technol.* **2003**, *20*, 466-477.

24. Barthelmie, R.J.; Larsen, G.C.; Frandsen, S.T.; Folkerts, L.; Rados, K.; Pryor, S.C.; Lange, B.; Schepers, G. Comparison of wake model simulations with offshore wind turbine wake profiles measured by SODAR. *J. Atmos. Ocean. Technol.* **2006**, *23*, 888-901.

25. Antoniou, I.; Jørgensen, H.E.; von Hünerbein, S.; Bradley, S.G.; Kindler, D. Inter-Comparison of Commercially Available SODARs for Wind Energy Applications. In *Proceedings of the 12th International Symposium on Acoustic Remote Sensing and Associated Techniques of the Atmosphere and Oceans*, Cambridge, UK, 11–16 July 2004.

26. Antoniou, I.; Jørgensen, H.E.; Bradley, S.G.; von Hünerbein, S.; Cutler, N.; Kindler, D.; de Noord, M.; Warmbier, G. The Profiler Intercomparison Experiment (PIE). In *Proceedings of the EWEA European Wind Energy Conference*, London, UK, 22–25 November 2004.

27. Bradley, S.G.; Antoniou, I.; von Hünerbein, S.; Kindler, D.; Jorgensen, H.; de Noord, M. *SODAR Calibration for Wind Energy Applications*; Final Report on WP3, EU WISE Project NNE5-2001-297; University of Salford: Greater Manchester, UK, 2005.

28. Hansen, K.S. Validation of SODAR Measurements for Wind Power Assessment. In *Proceedings of the EWEA European Wind Energy Conference*, Athens, Greece, 27 February–2 March 2006.

29. Behrens, P.; Bradley, S.; von Hünerbein, S. A scanning bi-static SODAR. *IOP Conf. Series: Earth Environ. Sci.* **2008**, *1*, 1-10.

30. Bradley, S.; von Hünerbein, S. Next-Generation Acoustic Wind Profilers. In *Proceedings of the EWEA European Wind Energy Conference*, Marseille, France, 16–19 March 2009.

31. National Renewable Energy Laboratory (NREL). *Comparison of Second Wind Triton Data with Meteorological Tower Measurements*; Report TP47429; NREL: Golden, CO, USA, 2010.

32. Verhoef, H.; van de Werff, A.; Oostrum, H. *Comparative Measurements between a Triton SODAR and Meteo Measurements at the EMTW, The Netherlands*; Report ECN-X--09-104; Energy Research Centre (ECN): Petten, The Netherlands, 2010.

33. Smith, D.; Harris, M.; Ciffey, A.; Mikkelsen, T.; Joergensen, H.; Mann, J.; Danielian, R. Wind LIDAR Evaluation at the Danish Wind Test Site in Høvsøre. In *Proceedings of the EWEA European Wind Energy Conference*, London, UK, 22–25 November 2004.

34. Deutsche WindGuard Consulting. *Evaluation of ZephIR*; Project No. VC 05250, Report PWG 06005; Deutsche WindGuard GmbH: Varel, Germany, 2006.

35. Jaynes, D.W. *MTC Final Progress Report—LIDAR*; Renewable Energy Research Laboratory, University of Massachusetts: Amherst, MA, USA, 2007.

36. Kindler, D.; Oldroyd, A.; MacAskill, A.; Finch, D. An eight month test campaign of the Qinetiq ZephIR system: Preliminary results. *Meteorologische Zeitschrift*, **2007**, *16*, 479-489.

37. Bradley, S.; von Hünerbein, S. Comparisons of New Technologies for Wind Profile Measurements Associated with Wind Energy Applications. In *Proceedings of the EWEA European Wind Energy Conference*, Milan, Italy, 7–10 May 2007.

38. Albers, A.; Janssen, A.W.; Mander, J. Comparison of LIDARs, German Test Station for Remote Sensing Devices. In P*roceedings of the German Wind Energy Conference, DEWEK 2008*, Wilhelmshaven, Germany, 26–27 November 2008.

39. Parmentier, R.; Cariou, J.; Sauvage, L.; Valla, M.; Lindelöw, P.; Antoniou, I. Accuracy and Relevance of Pulsed Doppler LIDAR Wind Profile Measurement in Complex Terrain. In *Proceedings of the EWEA European Wind Energy Conference*, Brussels, Belgium, 31 March–3 April 2008.

40. Courtney, M.S.; Wagner, R.; Lindelöw, P. Commercial LIDAR Profilers for Wind Energy—A Comparative Guide. In *Proceedings of the EWEA European Wind Energy Conference*, Brussels, Belgium, 31 March–3 April 2008.

41. Marti, I.; Gomez, P.; Jorgensen, H.E.; Courtney, M.S.; Harris, M. Comparison of LIDAR and Cup Anemometers in Complex Terrain. In *Proceedings of the EWEA European Wind Energy Conference*, Brussels, Belgium, 31 March–3 April 2008.

42. Peña, A.; Hasager, C.; Gryning, S.-E.; Courtney, M.; Antoniou, I.; Mikkelsen, T. Offshore wind profiling using light detection and ranging measurements. *Wind Energy* **2009**, *12*, 105-124.

43. Jaynes, D. LIDAR Validation and Recommendations for Wind Resource Assessments. In *Proceedings of the AWEA WINDPOWER 2009 Conference*, Chicago, IL, USA, 4–7 May 2009.

44. Wächter, M.; Gottschall, J.; Rettenmeier, A.; Peinke, J. Power Curve Estimation Using LIDAR Measurements. In *Proceedings of the EWEA European Wind Energy Conference*, Marseille, France, 16–19 March 2009.

45. Käsler, Y.; Rahm, S.; Simmet, R.; Kühn, M. Wake measurements of a multi-MW wind turbine with coherent long-range pulsed Doppler wind Lidar. *J. Atmos. Ocean. Technol.* **2010**, *27*, 1529-1532.

46. Courtney, M.; Lindelöw, P.; Wagner, R. LIDAR Profilers for Wind Energy—The Current Status. In *Proceedings of the EWEA European Wind Energy Conference*, Marseille, France, 16–19 March 2009.

47. Foussekis, D.; Georgakopoulos, T.; Karga, I. Investigating Wind Flow Properties in Complex Terrain Using 3 LIDARS and a Meteorological Mast. In *Proceedings of the EWEA European Wind Energy Conference*, Marseille, France, 16–19 March 2009.

48. Bingol, F.; Mann, J.; Foussekis, D. Lidar Performance in Complex Terrain Modelled by WASP Engineering. In *Proceedings of the EWEA European Wind Energy Conference*, Marseille, France, 16–19 March 2009.

49. Brady, O.; Harris, M.; Girault, R.; Abiven, C. Correction of Remote Sensing Bias in Complex Terrain Using CFD. In *Proceedings of the EWEA European Wind Energy Conference*, Warsaw, Poland, 20–23 April 2010.

50. Bouquet, M.; Parmentier, R.; Sauvage, L.; Cariou, J-P. Theoretical and CFD Analysis of Pulsed Doppler Lidar Wind Profile Measurement Process in Complex Terrain. In *Proceedings of the EWEA European Wind Energy Conference*, Warsaw, Poland, 20–23 April 2010.

51. Hu, C.-H. Applying CFD and Lidar for Wind Profiling and Risk Assessment in a Forested Area. In *Proceedings of the EWEA European Wind Energy Conference*, Warsaw, Poland, 20–23 April 2010.

52. Antoniou, I.; Jørgensen, H.E.; Mikkelsen, T.; Pedersen, T.F.; Warmbier, G., Smith, D. Comparison of Wind Speed and Power Curve Measurements Using a Cup Anemometer, a LIDAR and a SODAR. In Proceedings *of the EWEA European Wind Energy Conference*, London, UK, 22–25 November 2004.

53. Antoniou, I.; Courtney, M.; Jørgensen, H.E.; Mikkelsen, T.; von Hünerbein, S.; Bradley, S.; Piper, B.; Harris, M.; Marti, I.; Aristu, M.; Foussekis, D.; Nielsen, M.P. *Remote sensing the wind using Lidars and Sodars*; EU FP7 UPWIND Project, WP6; Risø National Laboratory for Sustainable Energy, Technical University of Denmark: Roskilde, Denmark, 2007.

54. Antoniou, I.; Jørgensen, H.E.; Mikkelsen, T.; Frandsen, S.; Barthelmie, R.J.; Perstrup, C.; Hurtig, M. Offshore Wind Profile Measurements from Remote Sensing Instruments. In *Proceedings of the EWEA European Wind Energy Conference*, Athens, Greece, 27 February–2 March 2006.

55. UpWind, EU FP6 Project. Remote Sensing papers and publications (Work Package 6). Available online: http://www.upwind.eu/publications/6-remote-sensing.aspx (accessed on 1 June 2011).

56. Hill, C.; Harris, M. *QinetiQ Lidar Measurement Report*; UpWind, EU Contract No. 019945 (SES6), 2010.

57. Lange, M.; Focken, U. *Physical Approach to Short-Term Wind Power Prediction*; Springer: Berlin, Germany, 2005; pp. 115-120.

58. Oldroyd, A. Preliminary Results of a Wind Industry Led Remote Sensing Intercomparison Study. In *Proceedings of the British Wind Energy Association 30th Conference*, London, UK, 21–23 October 2008.

Appendix

On-site atmospheric conditions were assessed in order to aid the understanding of the RS measurements, which were occasionally at odds with the cup anemometer measurements of wind speed. In addition, aviation METARS (Meteorological Aviation Routine Weather Report) data for Glasgow Airport, which is over 22 km from Myres Hill, were acquired and analyzed for the study period. The METARS data consists of twice-hourly automated meteorological measurements, and included barometric pressure, air and dew point temperatures; course estimates of visibility, clouds (e.g., 'few'); and the presence of various precipitation types. It was surmised that this data (although mainly of a qualitative nature) would provide some indication of atmospheric conditions in the region. In particular were those of interest to LIDAR, notably mist/fog and low-level clouds (the latter inferred from the 'overcast' flag).

Figure 12 is an example time series (March data of 10 min averages) of the measured meteorological parameters and the derived wind shear exponent, α. Strong wind shear (high α) is usually associated with very stable conditions. Figure 13 is a plot of a number of the Glasgow METARS parameters for the same period. Rain records are in broad agreement between the two sites (although not late in the month). However, comparison of the METARS data with the time series Cup, LIDAR and SODAR wind speeds illustrated in Figure 5, as well as the Lidar-Cup (or for that matter Sodar-Cup) wind speed differences shown in Figure 8, does not provide any robust explanation of the periods of significant differences between the RS instruments and the cup anemometer data, and this is most likely because of the substantial distance between Glasgow Airport and Myres Hill.

Figure 12. Selected meteorological characteristics for March 2008.
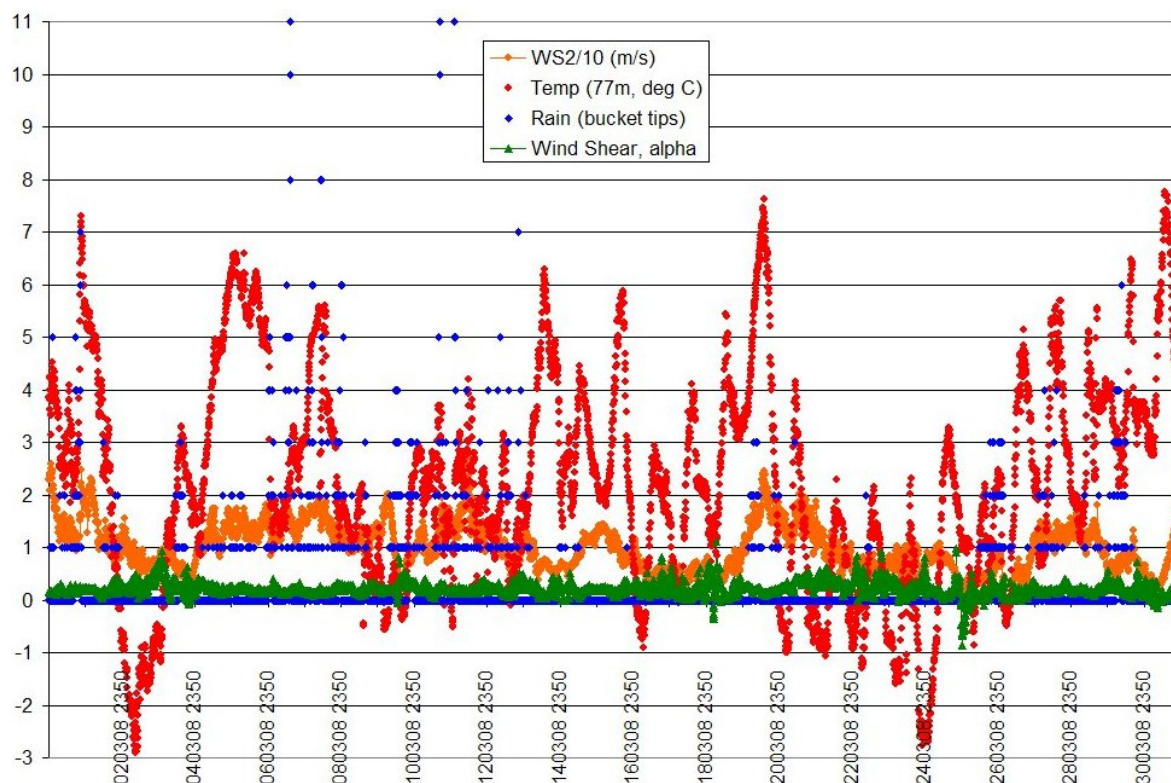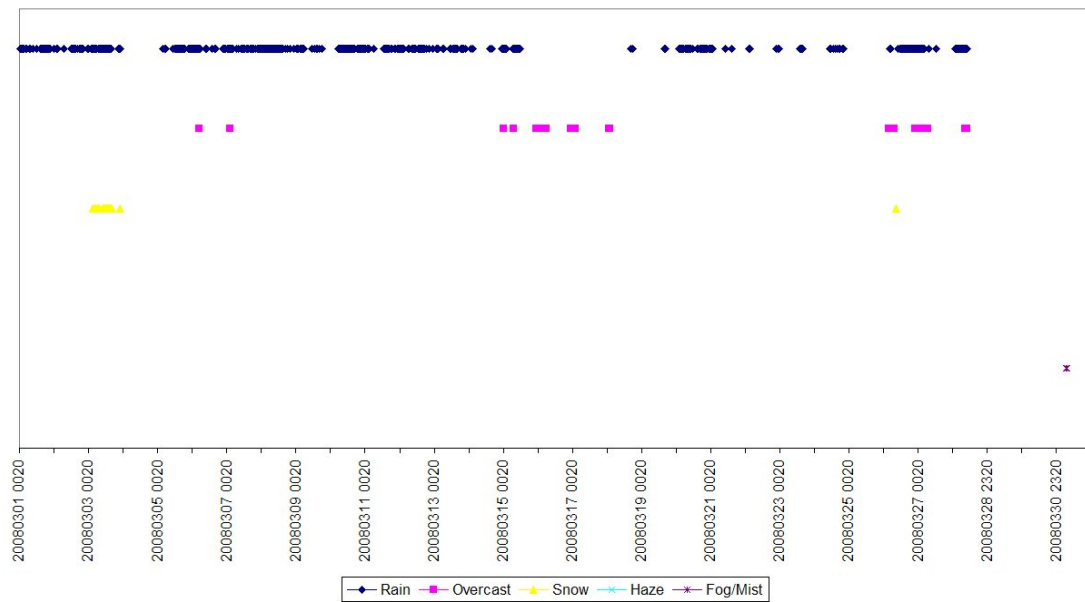
Figure 13. Selected Glasgow Airport METARS observations for March 2008.

The wind shear exponent, α, was calculated with the Power Law equation, using the cup wind speeds at 30 m (WS7) and 80 m (WS2): α = [log(WS2) − log(WS7)]/log(80/30). A further investigation of the wind speed differences between each RS instrument and the 80 m Cup anemometer data was carried out by comparing these to α, and these results are shown below in Figure 14. High wind shear (either positive or negative) was not particularly associated with large differences in wind speeds measured by cup anemometer and either of the RS instruments.

Figure 14. (**a**) LIDAR-Cup, and (**b**) SODAR-Cup, wind speed differences, as a function of wind shear exponent, α (February–May; 10 min averages).
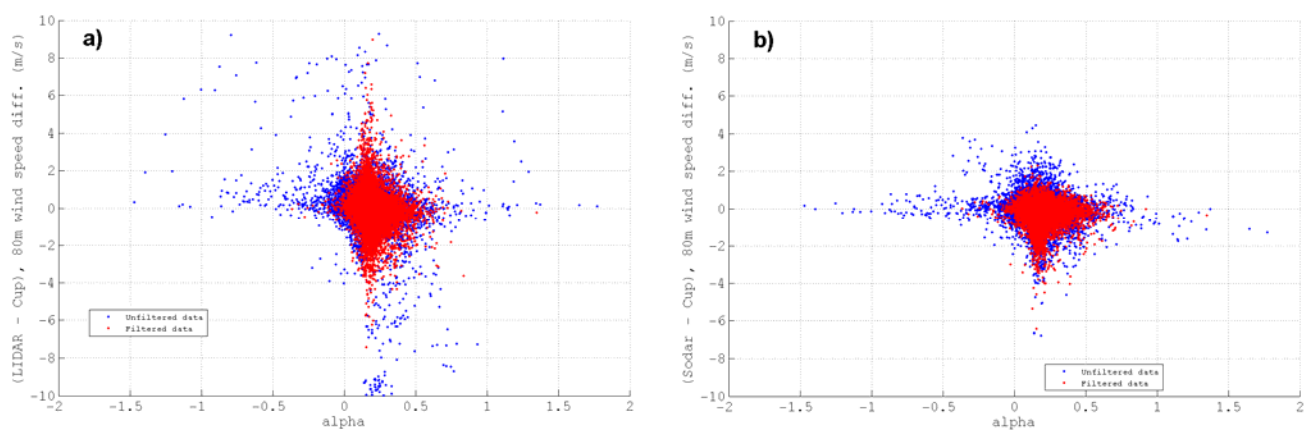
Meteorological Conditions during Measurement Program

Temperatures were mostly below 10 °C and rain was moderate during the second half of February. Some periods of negative wind shear (up to 1 m/s higher at 30 m, compared to 80 m) were recorded during calm periods, mainly in the middle of the month.

March was generally colder (8 °C maximum temperature at 77 m) and wetter, with only a few days in the middle of the month not recording any rain. Snow was observed on-site for a few days early in the month. Snow was also recorded during this period at Glasgow Airport. Strong wind shear was recorded during cold periods with very low winds (presumably very stable conditions), and this is illustrated in Figure 13.

The diurnal temperature cycle was more marked in April, along with generally higher temperatures and lower wind speeds than March. Rainfall was concentrated in the first half and the last week of the month. Negative shear again was mostly evident during calm periods.

May was significantly warmer and drier than the previous three months, with temperatures reaching 21 °C and only a few days recording any rainfall (albeit one very wet day on 10 May).